Review | Open Access

Journal of Materials Informatics

Chen *et al. J. Mater. Inf.* **2026**, *6*, 31 **DOI:**10.20517/jmi.2025.99

Computational strategies for the design of high-strength and high-thermal-conductivity casting Mg/Al alloys

Yunjian Chen[1], Ling Hu[1], Hongcan Chen[1], Kai Tang[2], Bin Liu[1], Yu Zhang[3], Bin Hu[4], Qun Luo[1,*], Qian Li[4,5,6,*]

Keywords:
Magnesium alloys, aluminum alloys, strength, thermal conductivity, design strategies

Citation: Chen, Y.; Hu, L.; Chen, H.; Tang, K.; Liu, B.; Zhang, Y.; Hu, B.; Luo, Q.; Li, Q. Computational strategies for the design of high-strength and high-thermal-conductivity casting Mg/Al alloys. *J. Mater. Inf.* **2026**, *6*, 31. https://dx.doi.org/10.20517/jmi.2025.99

Received: 31 Dec 2025
First Decision: 30 Jan 2026
Revised: 2 Mar 2026
Accepted: 20 Mar 2026
Published: 22 May 2026

Academic Editor:
Xiang-Dong Ding
Copy Editor:
Pei-Yun Wang
Production Editor:
Pei-Yun Wang

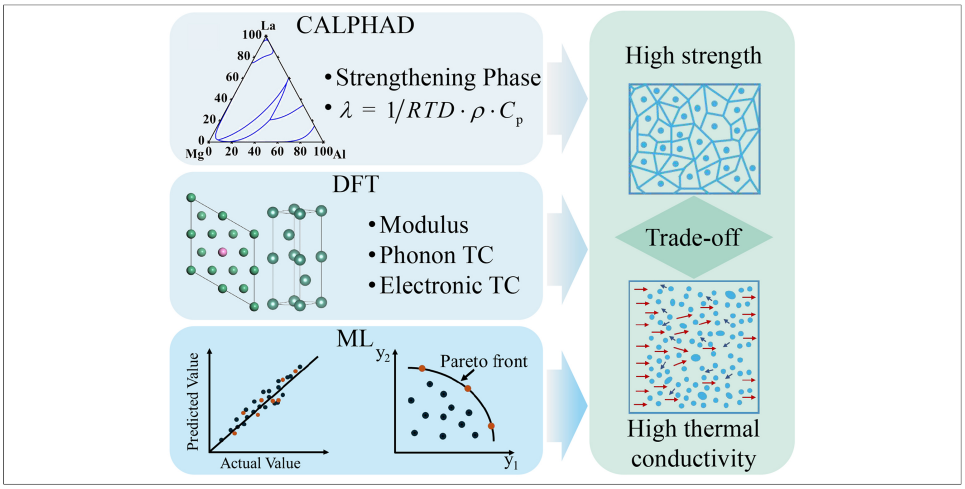

Abstract

High-strength and high-thermal-conductivity Mg/Al alloys are pivotal for lightweight thermal management applications in aerospace and electric vehicles, yet their development is hindered by the intrinsic trade-off between solute strengthening and electron scattering. This review summarizes the evolution of alloy design approaches from empirical trial-and-error methods to advanced artificial intelligence (AI)-driven strategies. First, the physical mechanisms governing strength and thermal conductivity (TC) are examined, identifying "matrix purification" and specific precipitation architectures as key microstructural design goals to minimize solute scattering. Then, the review critically evaluates traditional computational tools, including CALPHAD (CALculation of PHAse Diagrams) for phase equilibrium prediction and density functional theory for intrinsic

[1]State Key Laboratory of Materials for Advanced Nuclear Energy & School of Materials Science and Engineering, Shanghai University, Shanghai 200444, China.
[2]Department of Metal Production & Processing, SINTEF AS, Trondheim N-7034, Norway.
[3]International Joint Laboratory for Light Alloys (MOE), College of Materials Science and Engineering, Chongqing University, Chongqing 400044, China.
[4]Mingyue Lake Laboratory, Chongqing 401135, China.
[5]College of Materials Science and Engineering, National Engineering Research Center for Magnesium Alloys, National Key Laboratory of Advanced Casting Technologies, Chongqing University, Chongqing 400044, China.
[6]Henan Key Laboratory of Advanced Conductor Materials, Institute of Materials, Henan Academy of Sciences, Zhengzhou 450001, Henan, China.

***Correspondence to:** Prof. Qun Luo, State Key Laboratory of Materials for Advanced Nuclear Energy & School of Materials Science and Engineering, Shanghai University, Shanghai 200444, China. E-mail: qunluo@shu.edu.cn; Prof. Qian Li, College of Materials Science and Engineering, National Engineering Research Center for Magnesium Alloys, National Key Laboratory of Advanced Casting Technologies, Chongqing University, Chongqing 400044, China. E-mail: cquliqian@cqu.edu.cn

transport predictions. Crucially, we demonstrate that integrating these physics-based descriptors as input features into machine learning models significantly enhances prediction accuracy for complex multicomponent systems. Subsequently, the integration of these approaches for the concurrent optimization of strength and TC is discussed, highlighting the role of multi-objective optimization algorithms in mapping the Pareto frontier. Finally, the review discusses the future potential of emerging frontiers in Generative AI, such as generative adversarial networks (GANs), variational autoencoders (VAEs), and inverse design, highlighting the critical role of expert knowledge-guided constraints and physics-informed priors in steering model training and generation. Such hybrid frameworks are envisioned to autonomously navigate high-dimensional compositional spaces while maintaining physical interpretability and thermodynamic consistency, thereby accelerating the discovery of next-generation multifunctional alloys.

INTRODUCTION

The contemporary materials engineering landscape is defined by an uncompromising demand for multifunctionality. In the automotive, aerospace, and consumer electronics sectors, the era of selecting materials based on a single dominant property - be it strength, density, or thermal conductivity (TC) - has largely passed[1-3]. We are now in a regime of concurrent optimization, where structural components must effectively double as thermal management systems. For instance, electric vehicle (EV) battery enclosures require exceptional crashworthiness to protect volatile electrochemical cells while simultaneously dissipating the substantial heat generated during rapid charging cycles[4]. Magnesium (Mg) and aluminum (Al) alloys are natural candidates for these applications due to their lightweight nature (approximately 1.8 g/cm^3 for Mg alloys and 2.7 g/cm^3 for Al alloys). Notably, these cast alloys demonstrate a combination of high ultimate tensile strength (UTS), exceeding 300 and 350 MPa, and excellent TC, surpassing 150 and 220 W/(m·K) for Mg and Al alloys, respectively [Figure 1][5-8].

However, a fundamental physical contradiction lies at the heart of their development: the microstructural features required to strengthen these alloys are inextricably linked to the mechanisms that degrade their TC. Strength enhancement is typically realized by introducing microstructural defects such as solute atoms, precipitates, or grain boundaries to impede dislocation motion, thereby improving mechanical performance. However, these defects inevitably act as electron-phonon scattering centers, leading to a pronounced reduction in TC[9-12]. This intrinsic negative correlation between strength and TC gives rise to a natural performance trade-off in multi-objective alloy design. Consequently, breaking this trade-off and realizing the concurrent optimization of strength and TC not only demands precise control over the type, size, and distribution of second phases, but also requires a holistic consideration of multiple strengthening mechanisms, including solid-solution strengthening, precipitation strengthening, and grain boundary engineering. This challenge has emerged as a critical bottleneck in the development of high-performance Mg and Al alloys, as well as other lightweight metallic materials.

Historically, navigating this "strength-conductivity trade-off" has been an exercise in empirical persistence (trial and error), a strategy limited by high costs and long development cycles[13]. Although the CALPHAD (CALculation of PHAse Diagrams) approach can be applied to predict phase constitution and microstructural evolution, thereby assisting in the design of strengthening precipitates and thermally conductive phases, and density functional theory (DFT) can evaluate the strength and thermal transport properties of individual systems at the atomic scale to provide theoretical guidance for the design of high-strength and high-thermal-conductivity alloys, these computational methods have largely been employed as auxiliary tools within traditional research frameworks and have not yet been systematically integrated. When addressing conflicting properties such as strength and TC, conventional methods often only achieve improvements in a single property or simple compromises among multiple properties.

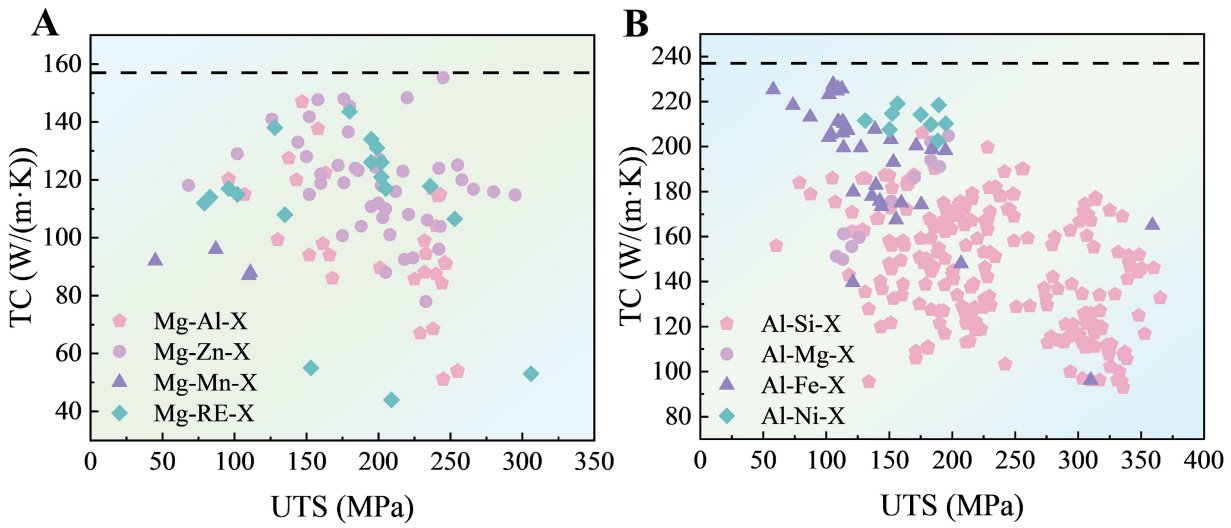

Figure 1. The UTS and TC of (A) cast Mg alloys and (B) cast Al alloys. Adapted from Ref.[8]. Copyright 2024, OAE Publishing Inc. UTS: Ultimate tensile strength; TC: thermal conductivity.

Moreover, it remains difficult to accurately elucidate the complex mapping relationships within the composition-processing-microstructure-performance (CPSP) framework, making it impossible to find globally optimal solutions.

In response to the challenges associated with traditional methods, the materials informatics paradigm centered on machine learning (ML) offers a transformative path forward[14,15]. Its core value lies in transforming materials research and development from an experience-driven model to an efficient data-driven paradigm[16,17]. By deeply mining existing experimental and simulation data, ML algorithms can effectively decipher the complex, high-dimensional, and nonlinear intrinsic relationships within the CPSP framework of alloys[18,19]. This enables researchers to conduct large-scale virtual screening and quickly evaluate tens of thousands of potential alloy compositions and processing combinations, greatly reducing the cycle time and cost of experimental verification. Therefore, ML has not only accelerated the research and development process of high-performance Mg/Al alloys, but has also made it possible to achieve synergistic optimization of multiple conflicting properties such as strength and TC. Despite the widespread application of these computational methods in alloy design, systematic integration has yet to be achieved in the design of high-strength and high-thermal-conductivity Mg/Al alloys.

This review provides a critical analysis of computational strategies for designing high-strength and high-thermal-conductivity Mg/Al alloys. First, we dissect the physical basis of the strength-conductivity conflict by analyzing strengthening mechanisms alongside electron and phonon transport behaviors. We then compare single-objective methodologies - from rigorous CALPHAD and DFT thermodynamics to rapid ML predictions. The core of our analysis focuses on Multi-Objective Optimization frameworks that explicitly map the Pareto frontier of optimal compromises. Finally, we explore the emerging frontier of generative artificial intelligence (AI), such as generative adversarial networks (GANs), variational autoencoders (VAEs), and inverse design, positing a future where alloys are not merely screened but autonomously generated by computational agents. The success of this transition hinges on human-centric decisions, specifically the expert-driven establishment of high-fidelity datasets to ensure that AI-generated designs remain grounded in scientific reality.

PHYSICAL BASIS OF STRENGTH AND TC

Strengthening mechanisms

As lightweight structural metals, the key to strength enhancement in Mg and Al alloys lies in establishing a multi-scale barrier system within the microstructure through alloy design and processing techniques, thereby effectively hindering dislocation movement and improving alloy strength. These strengthening mechanisms mainly include grain refinement strengthening, solid solution strengthening, precipitation strengthening, and dislocation strengthening. Essentially, these mechanisms introduce corresponding microstructural features into the matrix, such as grain boundaries, solute atoms, second-phase particles, and high-density dislocations. These multi-scale obstacles act synergistically to provide strong resistance to dislocation movement, ultimately enhancing the strength and hardness of the alloys. The total yield strength (YS) of the alloy is expressed as[20]:

$$\sigma_{\text{total}} = \sigma_0 + \sigma_{ss} + \sigma_{gs} + \sigma_{PPT} \tag{1}$$

where σ_0 is the yield stress of the pure alloy, σ_{ss} is solid solution strengthening, σ_{gs} is grain size strengthening, and σ_{PPT} is precipitation strengthening.

Solid solution strengthening

Solid solution strengthening refers to the addition of solute atoms to a metal matrix to form a solid solution, causing lattice distortion and thereby increasing the resistance to slip of dislocations in the lattice, which improves the strength of the material[21,22]. The variation in solid solution strengthening (σ_{ss}) with solute concentration can be expressed as follows[23]:

$$\sigma_{ss} = K \cdot C^m \tag{2}$$

where C is the atomic concentration of the solute, and K and m are constants related to the properties of the matrix and alloying elements; the value of m ranges from 0.5 to 1. Based on known element interaction mechanisms, the proportions of major alloying elements, trace elements, and impurity elements are selected and adjusted to design the alloy composition. Various alloying and microalloying elements, such as Ce, Nd, Y, Si, Ca, Ti, B, Sr, Sb, Bi, and Pr, have been demonstrated to enhance the mechanical properties of AZ91 and AM60 alloys. Among these elements, Ce, Nd, Y, Bi, and Sb are particularly effective in improving the tensile performance of AZ91 and AM60 alloys[24-26].

Grain refinement strengthening

The classic Hall-Petch relationship is used to describe the relationship between grain size and strength[27]:

$$\sigma_{gs} = k \cdot d^{-1/2} \tag{3}$$

where d is the average grain diameter, and k is the stress concentration factor of grain boundaries acting as slip obstacles. Grain refinement is mainly achieved by promoting nucleation and controlling solid-state phase transformations[28-30]. The core principle is to promote nucleation while suppressing grain growth, thereby enabling grain boundaries to act as effective barriers to dislocation motion, which enhances strength while maintaining toughness. In cast Mg/Al alloys, grain refinement is generally achieved by adding refiners, which increase the number density of heterogeneous nucleation sites during solidification, thereby enhancing the mechanical properties of the alloy. The most common chemical grain refinement approaches are Zr addition[31-34] and Al addition[35-38]. In cast Al alloys, the most common chemical grain refinement approaches are Al-Ti-B addition[39] and Al-Ti-Nb-B addition[40].

Precipitation strengthening

Precipitation strengthening is achieved through the formation of finely dispersed second-phase particles within the metallic matrix, which impede dislocation motion either by forcing dislocations to shear the precipitates or by causing them to bypass the precipitates through the Orowan mechanism, thereby significantly enhancing the strength of the material[41].

$$\sigma_{PPT} = \frac{Gb}{2\pi\lambda\sqrt{1-\nu}}\ln\frac{d_{\mathrm{p}}}{r_0} \tag{4}$$

where G is the shear modulus of the Mg matrix phase, b is the magnitude of the Burgers vector of gliding dislocations in Mg, ν is Poisson's ratio, λ is the effective planar interparticle spacing, d_{p} is the mean planar diameter of the particles, and r_0 is the core radius of the dislocations. This mechanism is considered a standard strategy for designing materials with high TC: precipitating solute atoms out of the matrix purifies the lattice for electron transport, while the precipitates simultaneously provide strengthening.

In the shear mechanism, dislocations interact with shearable precipitates through a variety of mechanisms, giving rise to distinct strengthening effects. The primary types include chemical (interfacial) strengthening, stacking-fault strengthening, modulus strengthening, coherency strengthening, and order strengthening. This relationship can be simply expressed as follows[42]:

$$\Delta\tau = \frac{2}{L_P b\sqrt{\Gamma}}\cdot\left(\frac{F}{2}\right)^{3/2} \tag{5}$$

where Γ is the dislocation line tension in the Mg matrix, F is a measure of the resistance of the precipitates to dislocation shearing, and L_p is the dislocation pile-up length. The CRSS contributed by shearable precipitates is related to Γ and F. Consequently, for given precipitates and dislocation types, the precipitate size determines which interaction mechanism is activated. Precipitates smaller than a critical size undergo the shearing mechanism, whereas those larger than the critical size are bypassed.

Dislocation strengthening

Strain hardening arises during plastic deformation as the density of dislocations increases, leading to enhanced dislocation interactions and entanglements that impede further dislocation motion and consequently increase the flow stress and strength of the material[43]. In industrial production, this strengthening effect is mainly achieved through cold working processes such as cold rolling, cold drawing, forging, and stamping. As this work primarily focuses on casting alloys, this section is not discussed further.

TC mechanism

The total TC of an alloy consists of two parts: electronic TC (k_e) and phonon TC (k_p), with electronic heat conduction being the dominant mechanism. Figure 2A shows the microscopic physical processes in which electrons and phonons participate in thermal and electrical conduction, respectively[44]. Based on a first-principles calculation framework incorporating electron–phonon coupling, the electron and phonon TCs of more than a dozen metals and intermetallic compounds at room temperature were calculated by considering electron–phonon interactions, as illustrated in Figure 2B[45]. The results indicate that the electronic TCs of Mg and Al account for 96.14% and 97.60% of their total TCs, respectively. In contrast, in transition metals and intermetallic compounds, stronger electron–phonon coupling leads to a more significant reduction in electronic TC, thereby increasing the relative contribution of phonons[45].

Alloying enhances the strength of alloys while reducing their TC. The fundamental reason is that the microdefects introduced during alloying hinder dislocation movement while simultaneously scattering electrons and phonons, thereby impeding their directional transport. From a microscopic perspective, the

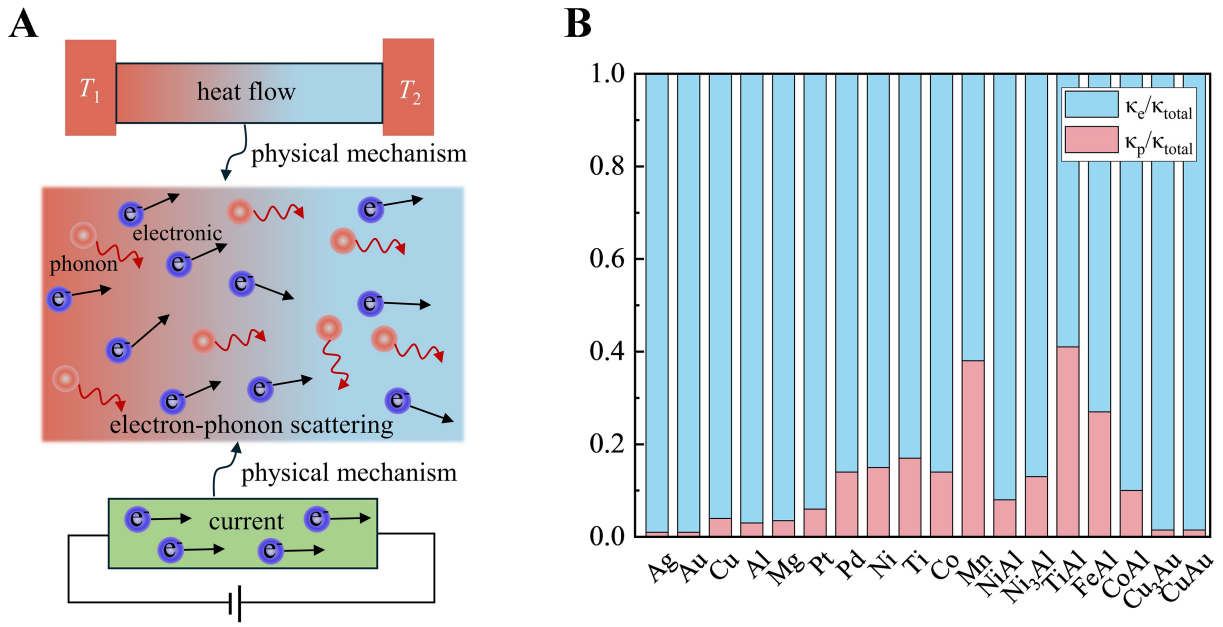

Figure 2. (A) Schematic diagram of the microscopic processes involved in thermal and electrical conduction in metals. Adapted from Ref.[44]. Copyright 2024, Science Press; (B) Contributions of electron and phonon TC to the total TC of metals below 300 K. Adapted from Ref.[45]. Copyright 2019, American Physical Society. TC: Thermal conductivity.

main factors that reduce TC include solute atoms, second phases, grain boundaries, dislocations, and defects[44,46]. Figure 3 shows the four factors affecting TC.

Solute atoms

Solute atoms, acting as point defects, disrupt the long-range periodicity of the crystal lattice and give rise to elastic scattering of charge carriers, thereby reducing the electronic contribution to TC. When alloying elements are dissolved into the Mg/Al matrix in the form of solute atoms, the associated atomic size mismatch and local bonding perturbations induce lattice distortions and elastic strain fields. These distortions serve as effective scattering centers for both electrons and phonons, impeding their coherent transport through the lattice, shortening the carrier mean free path, and ultimately leading to a pronounced degradation of TC. Moreover, as the solute concentration increases, the cumulative scattering effect becomes increasingly significant[47], further exacerbating the trade-off between alloying-induced strengthening and heat transport efficiency.

The TC of Mg/Al alloys decreases with increasing solute atom content, and different solute atoms exert varying degrees of influence on TC. Figure 4A shows the variation in TC of binary Mg alloys with different solute elements and concentrations[48]. It can be observed that the addition of alloying elements reduces the TC of Mg alloys. At low alloying concentrations, the relationship between composition and TC is approximately linear[48]. However, once the maximum solubility limit is exceeded, the linear trend deviates and the slope decreases. The weakening effects of common alloying elements (Zn, Al, Ca, Sn, Mn, Zr) on the TC of Mg alloys follow the order: Zr > Mn > Sn > Ca > Al > Zn. Figure 4B shows the variation in the electrical conductivity of binary Al alloys with different solute elements and concentrations. It can be seen that the electrical conductivity of Al decreases with increasing alloying element content in solid solution, and different alloying elements exert different inhibitory effects. The weakening effects of common alloying elements (Si, Cu, Mg, Zn) on the TC of Al follow the order: Si > Mg > Cu > Zn, while trace elements such as Cr, V, Mn, Ti, and Li exhibit much stronger suppressing effects[49]. Similar results have also been observed for the TC of binary Al alloys[50].

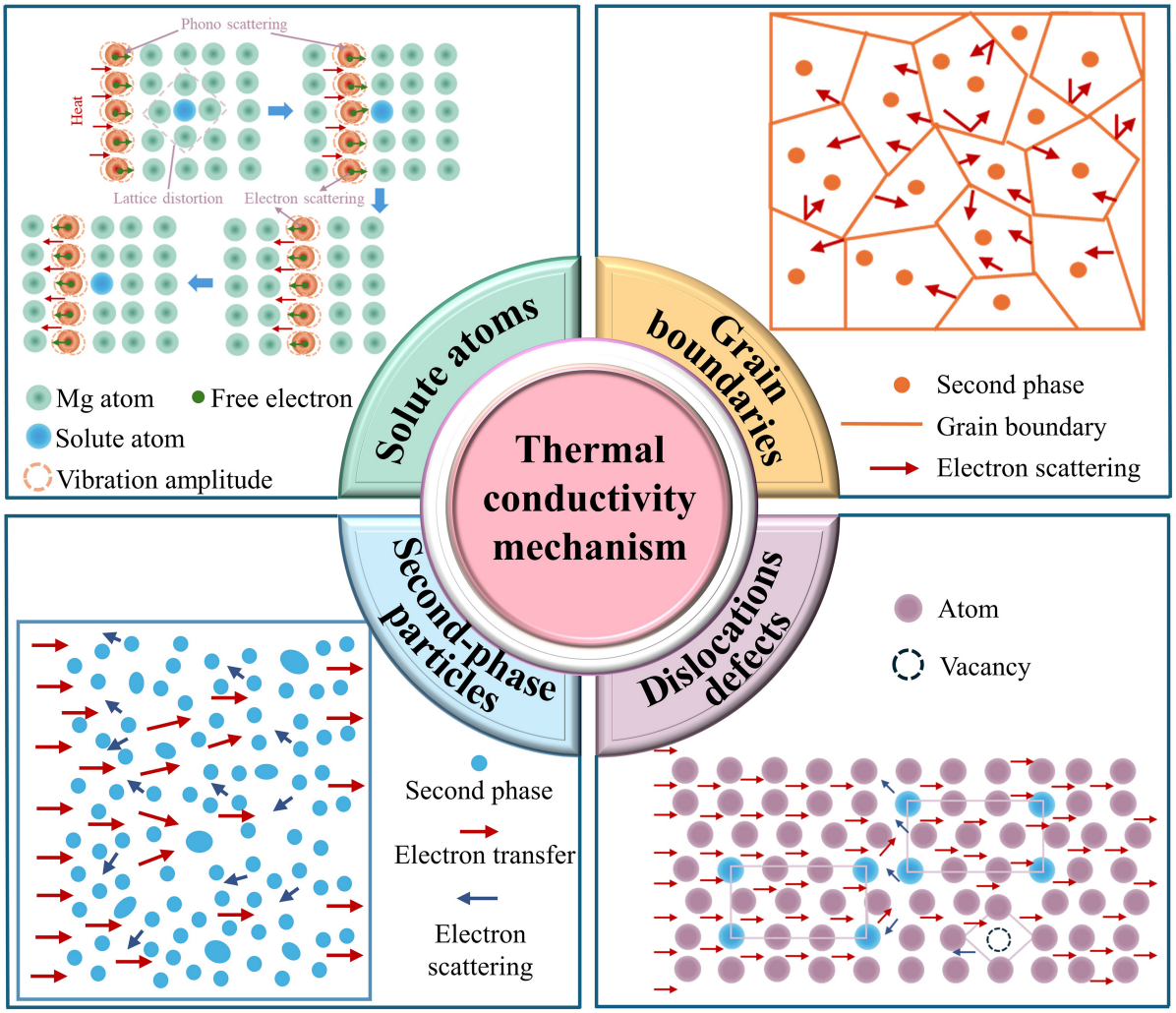

Figure 3. Factors affecting TC. TC: Thermal conductivity.

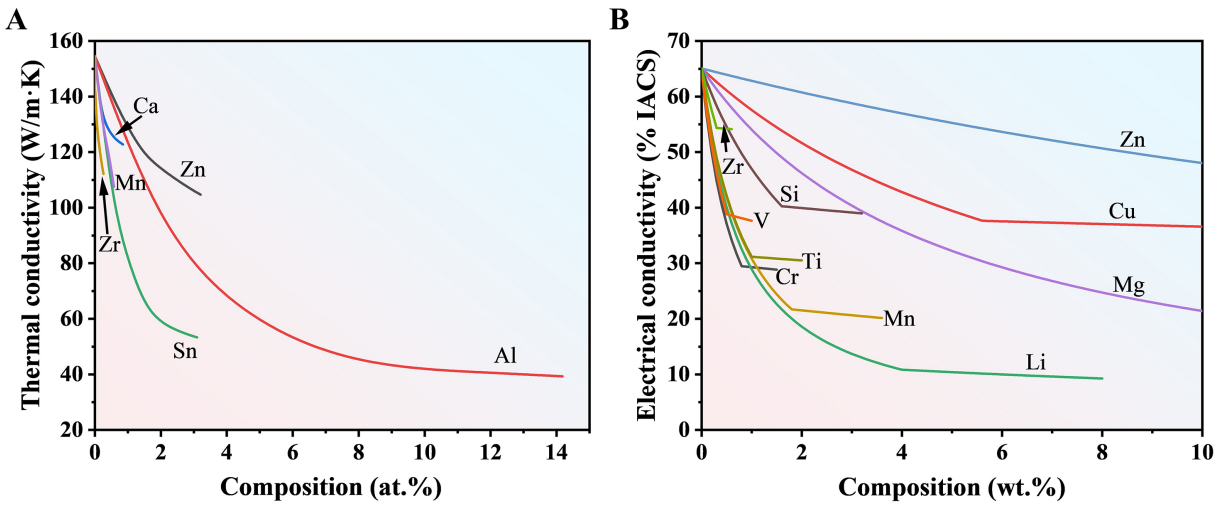

Figure 4. Variation in (A) the TC of binary Mg alloys and (B) the electrical conductivity of binary Al alloys with solute concentration. Adapted from Ref.[49]. Copyright 2024, Elsevier. TC: Thermal conductivity; IACS: International Annealed Copper Standard.

Second phases

Second-phase particles act as physical obstacles to charge transport, introducing both elastic and inelastic scattering events that hinder electron mobility and consequently reduce the electronic contribution to TC[51]. The precipitation of second phases inevitably generates additional phase interfaces. Owing to lattice parameter mismatches between the intermetallic compounds and the Mg matrix, localized lattice distortions and interfacial strain fields are formed in the vicinity of these interfaces[52]. Nevertheless, in contrast to solute atoms that are randomly distributed throughout the matrix, the lattice distortions induced by well-defined intermetallic compounds are spatially confined and structurally ordered. As a result, their overall scattering efficiency for electrons and phonons is comparatively limited. When an equivalent amount of alloying elements is introduced, solute atoms dissolved in the matrix exert a substantially stronger influence on both electrical and thermal resistivity than that arising from the formation of second-phase particles, primarily due to their pervasive distribution and cumulative scattering effects[44,46,47]. This distinction highlights the critical role of solute state and phase morphology in regulating heat and charge transport in Mg/Al alloys.

For as-cast and solution-treated Mg–La, Mg–Ce, Mg–Sm, and Mg–Al alloys, the relationship between TC and the nominal concentration of excess secondary phases was fitted using the least-squares method, yielding conductivity–excess phase concentration curves[53]. The TC of the solution-treated alloys was lower than that of the as-cast alloys, and the absolute value of the slope increased. This may be attributed to the decomposition of secondary phases during solution treatment, leading to the diffusion of alloying atoms into the Mg matrix. These results further indicate that solute atoms exert a greater influence on TC than second phases. Figure 5 presents the experimental thermal diffusivities of the as-cast Mg-Zn-La/Ce alloys[54]. A comparison of Figure 5A and C reveals that the thermal diffusivity of the alloy containing the $LaMg_{12}$ phase is approximately 11.8-15.4 mm^2/s higher than that of the alloy containing the τ_1 phase, indicating that the τ_1 phase exerts a more detrimental effect on the thermal diffusivity of Mg alloys than $LaMg_{12}$. A similar trend is observed in the Mg-Zn-Ce system [Figure 5B and D], where the thermal diffusivity of the $CeMg_{12}$-containing alloy is 2.5-3.6 mm^2/s higher than that of its τ_1-containing counterpart. To design Mg and Al alloys with high TC, the solute content in the matrix should be minimized. By introducing sacrificial elements, detrimental solute atoms can be precipitated as separate second phases, which effectively reduces lattice distortion and enhances overall TC.

Grain boundaries

Grain boundaries are planar defects characterized by disrupted atomic periodicity and locally disordered atomic configurations. The breakdown of lattice continuity at grain boundaries gives rise to mismatch-induced strain fields and vibrational disorder, which act as effective scattering centers for both electrons and phonons, thereby suppressing thermal transport[55,56]. As the grain size decreases, the volume fraction and density of grain boundaries increase markedly, leading to more frequent electron–boundary interactions and enhanced carrier scattering. In particular, phonons, whose mean free paths are often comparable to or larger than typical grain sizes, are strongly affected by grain boundary scattering. Grain refinement therefore results in a pronounced reduction in lattice TC, especially at intermediate and low temperatures where phonon transport dominates. These effects underscore the critical role of grain size engineering in balancing mechanical strengthening and TC in Mg/Al alloys. Tong *et al.* investigated the effect of grain size on the TC of as-cast pure Mg and found that the TC increased with increasing grain size[57].

Dislocations

Dislocations, as line defects associated with long-range strain fields and localized lattice distortions, act as effective scattering centers for both electrons and phonons[58]. For electrons, strain-induced perturbations of the periodic potential lead to enhanced elastic scattering, resulting in increased electrical resistivity and a

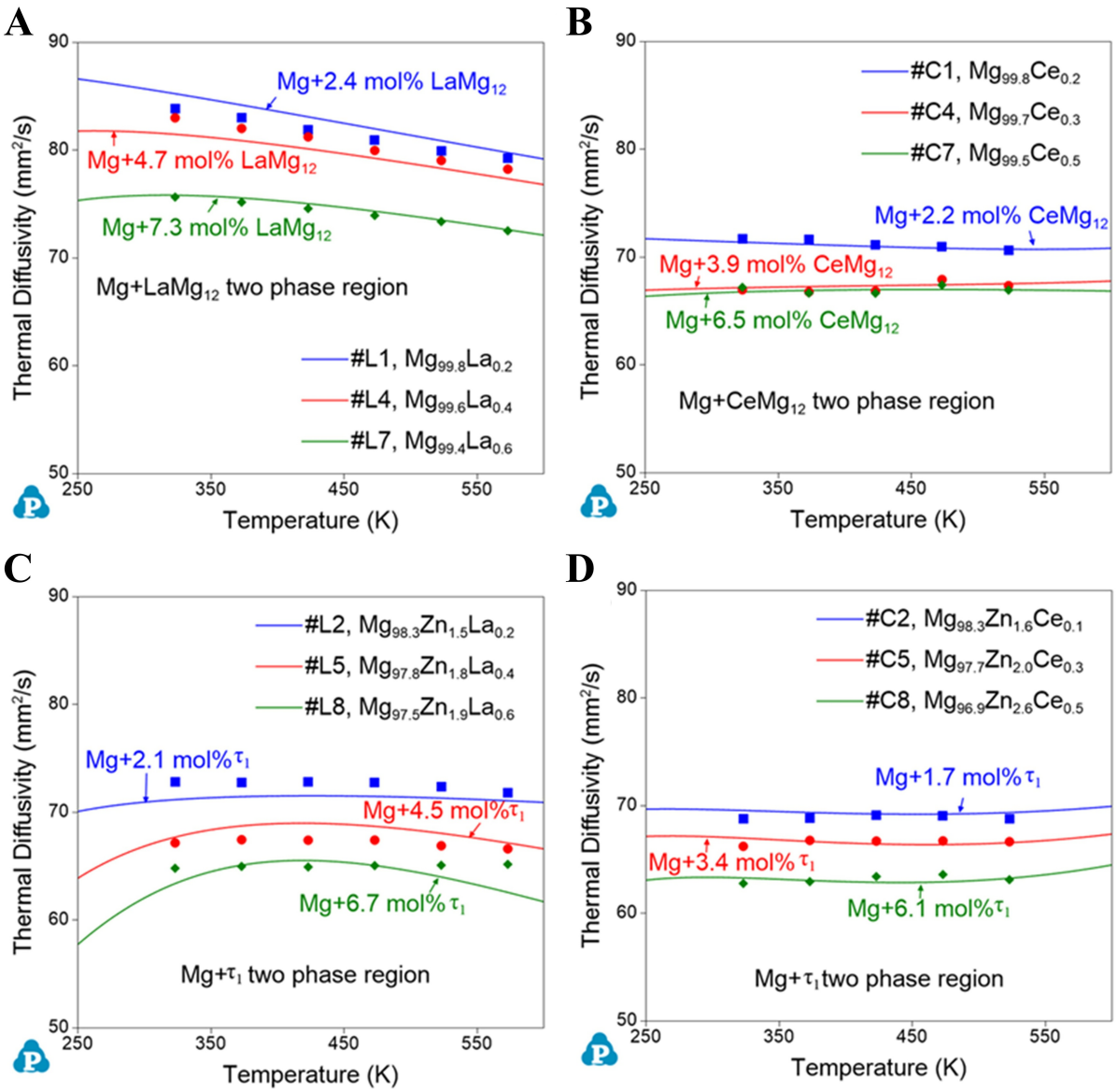

Figure 5. Thermal diffusivities of as-cast (A and C) Mg–Zn–La and (B and D) Mg–Zn–Ce alloys. Adapted from Ref.[54]. Copyright 2022, Elsevier.

corresponding reduction in the electronic contribution to TC. For phonons, the dislocation core and its surrounding strain field disrupt lattice vibrational coherence, strongly impeding phonon propagation and shortening the phonon mean free path, thereby degrading lattice TC. The influence of dislocations on thermal transport is particularly pronounced in deformed or heavily strengthened alloys, where high dislocation densities amplify carrier scattering effects and exacerbate the trade-off between mechanical strengthening and TC.

SINGLE-OBJECTIVE DESIGN OF HIGH-STRENGTH AND HIGH-THERMAL-CONDUCTIVITY Mg/Al ALLOYS

Design of high-strength Mg/Al alloys

CALPHAD and DFT have become major pillars of computationally assisted alloy design. With the rapid advancement of computational materials science, ML is emerging as a new paradigm for materials design. The CALPHAD method, centered on thermodynamic databases, enables the calculation of critical

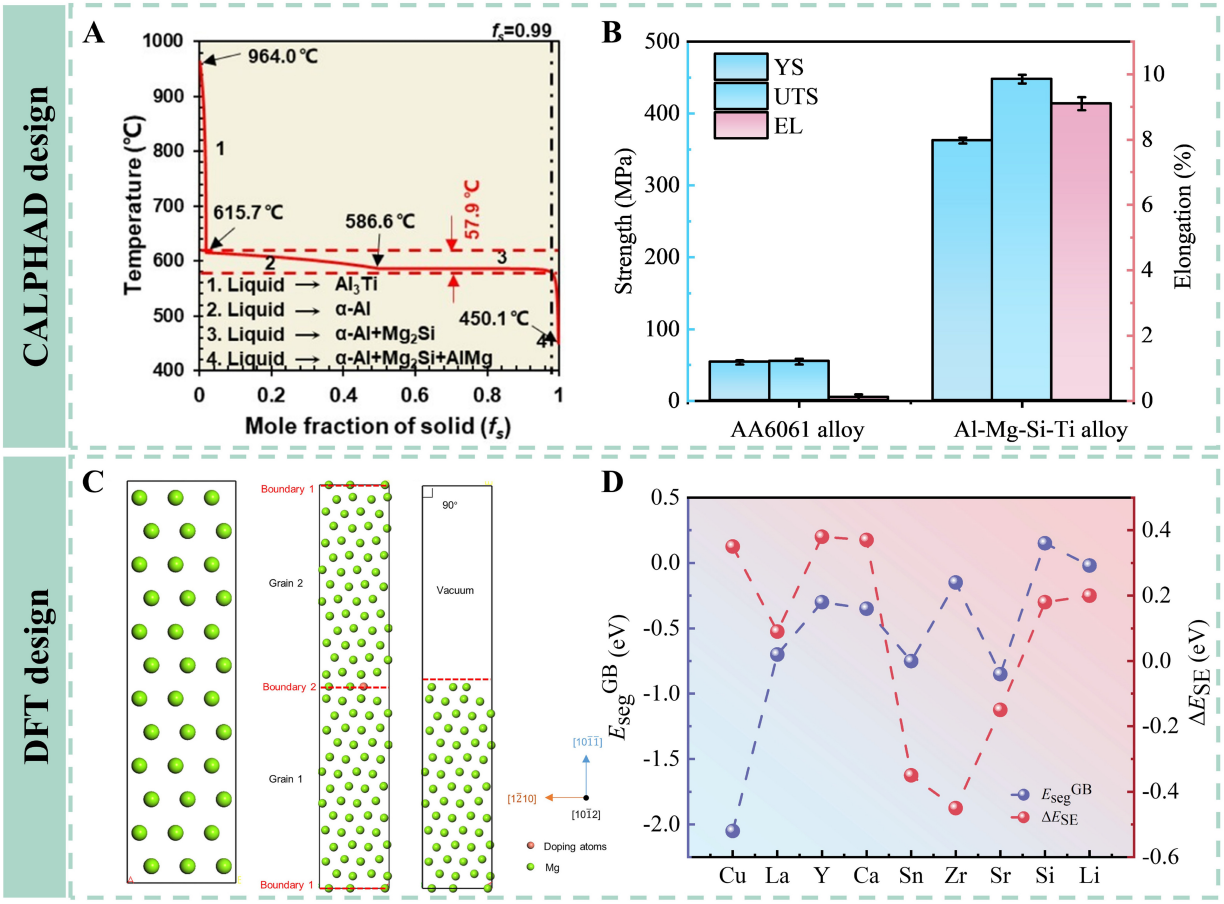

Figure 6. CALPHAD- and DFT-assisted design of strengthened alloys. (A) Solidification paths of the Al-Mg-Si-Ti alloy calculated using the Scheil-Gulliver model; (B) Mechanical properties of AA6061 and Al-Mg-Si-Ti alloys. (A and B) adapted from Ref.[63]. Copyright 2024, Taylor and Francis Ltd; (C) 3 × 3 × 6 Mg supercell model, twin boundary model, and free-surface model; (D) Calculation results for Mg twin boundaries doped with common alloying elements. (C and D) adapted from Ref.[67]. Copyright 2025, Nonferrous Metals Society of China. CALPHAD: CALculation of PHAse Diagrams; DFT: density functional theory; YS: yield strength; UTS: ultimate tensile strength; EL: elongation.

parameters such as solidification pathways, equilibrium phase constitutions, and phase fractions[59-61]. This provides a quantitative basis for tailoring the type and volume fraction of secondary phases, as well as for assessing the potential contributions of solid-solution and second-phase strengthening. By incorporating expert domain knowledge, this approach streamlines the design process by prioritizing these dominant strengthening contributors, thereby providing a focused strategic framework for the compositional design of high-strength Mg/Al alloys. For example, by employing the CALPHAD approach to construct the Al–Fe–Si ternary phase diagram, the mechanical properties of key secondary phases can be systematically investigated[62]. Through directional solidification, millimeter-scale particles were prepared, and the elastic moduli of the α-AlFeSi, β-AlFeSi, and Mg_2Si phases were successfully measured to be 183.81 ± 8.64, 174.13 ± 6.81, and 116.38 ± 4.06 GPa, respectively. The corresponding Vickers hardness values were 883 ± 64, 765 ± 21, and 475 ± 22 HV. Notably, α-AlFeSi exhibited more pronounced hardness anisotropy than β-AlFeSi, reflecting differences in crystal structure and bonding characteristics. The CALPHAD approach was also utilized to assist in the design of a high-strength and crack-free Al-Mg-Si-Ti alloy. The solidification pathway of the Al-Mg-Si-Ti alloy was calculated using the Scheil-Gulliver model [Figure 6A]. The Al_3Ti phase formed during the initial stage of solidification, whereas the Mg_2Si phase began to precipitate when the solid fraction (fs) reached 49.7%. Owing to its low lattice mismatch with the α-Al matrix and high growth restriction factor, the Al_3Ti phase effectively refined the grains. Compared to the AA6061 alloy, the designed Al-Mg-Si-Ti alloy exhibited a high YS of 362.4 MPa, a UTS of 447.8 MPa, and an El of 9.1% [Figure 6B], successfully maintaining an excellent strength-ductility synergy[63].

These results demonstrate the capability of CALPHAD-based thermodynamic modeling to guide the identification of strengthening phases for the design of high-strength alloys[60,62]. However, despite its effectiveness in predicting phase stability and composition, the CALPHAD framework remains limited in directly predicting mechanical strength, underscoring the need for its integration with data-driven and physics-informed materials informatics approaches. It should be emphasized that CALPHAD is inherently an expert knowledge-driven methodology that relies on physically grounded thermodynamic models, assessed databases, and metallurgical experience to encode phase equilibria and transformation behaviors, thereby providing a reliable foundation for coupling with ML and multiscale modeling strategies.

The DFT method operates at the atomic and electronic scales, enabling first-principles calculations of electronic structure, phase stability, and intrinsic elastic properties. By explicitly resolving atomic bonding characteristics and electronic interactions, DFT provides quantitative insights into structure–property relationships that are difficult to access experimentally[64,65]. It elucidates the fundamental physical mechanisms of alloy strengthening and enables the targeted design of strengthening phases. Systematic DFT calculations have revealed that while the solid-solution strengthening of solute elements X (X = Li, Al, Mn, Zn, Y, Zr, Nd, Gd) in Mg alloys primarily originates from lattice distortion with an intensity order of Mn > Nd > Gd > Y > Zn > Al > Zr > Li, the local ordering of Mg–X complexes becomes the dominant governing factor at higher solute concentrations[66]. Zhou *et al.* successfully designed and synthesized low-cost, high-performance Mg–10Zn–4Al–0.4Mn-*x*Sn (x = 0.0, 0.2, 0.4, 0.6) alloys by regulating the τ-Mg_{32} (Al, Zn)$_{49}$ phase and optimizing the twin boundaries through DFT calculations. Figure 6C illustrates the Mg supercell model and the constructed $\{10\bar{1}2\}$ twin boundary model. By calculating the segregation energies of various doping atoms at Mg twin boundaries [Figure 6D], the authors demonstrated that all alloying elements except Si could stably segregate to the boundaries. However, only Sn, Zr, and Sr exhibited negative segregation energies, suggesting that their segregation effectively enhances boundary strength. The strengthening effectiveness followed the order of Zr > Sn > Sr[67]. Moreover, DFT-derived quantities, such as formation energies, elastic constants, density of states, and charge density distributions, serve as physically meaningful descriptors in materials informatics workflows, thereby supporting data-driven modeling and the rational design of advanced alloys.

The ML method is inherently data-driven, integrating large and heterogeneous datasets encompassing alloy compositions, processing parameters, as well as mechanical and TC properties. By learning complex, high-dimensional correlations from experimental and computational data, ML models enable rapid prediction of material performance and efficient exploration of composition-process-property spaces[68-70]. These data-driven correlations, extracted through advanced algorithms, facilitate the construction of accurate predictive models, thereby enabling accelerated screening and optimization of alloy compositions. A Mg alloy database was developed, and twelve ML models were trained for the prediction and discovery of Mg alloys with superior mechanical properties[71]. Based on the optimal gradient boosting regression (GBR) model, an Adaptive Synthetic Minority Over-sampling Technique (A-SMOTE) algorithm was employed to balance the data distribution. By further incorporating solubility constraints, an inverse design strategy was implemented, ultimately enabling the design of high-strength Mg alloys. Zhu *et al.* developed a multimodal fusion learning framework that integrates image processing and ML techniques to construct a multimodal dataset combining textual information and microstructural images[72]. Based on this dataset, ML models were successfully trained to predict the mechanical performance of high-strength Al alloys. This approach enabled a systematic exploration of composition-microstructure-property relationships, demonstrating the potential of multimodal data-driven strategies for advanced alloy design[72]. However, throughout the ML process, expert knowledge must be incorporated to identify microstructures requiring analysis. This involves translating microstructural information into features that are recognizable by ML models, enabling subsequent model construction and prediction.

Design of high-thermal-conductivity Mg/Al alloys

The design philosophy of high-thermal-conductivity Mg and Al alloys is opposite to that of high-strength alloys. While high-strength alloys achieve strengthening by introducing various microstructural obstacles - such as solute atoms, grain boundaries, and precipitates - to impede dislocation motion, high-thermal-conductivity alloys instead aim to minimize microstructural defects to reduce the scattering of heat carriers, including electrons and phonons. This intrinsic trade-off poses a significant challenge for the simultaneous optimization of mechanical and thermal properties. The CALPHAD method has been successfully applied to the calculation of TC in Mg and Al alloys[73,74]. The incorporation of TC parameters into thermodynamic databases has enabled quantitative prediction of heat transport properties in multicomponent alloy systems. For instance, reliable computational models have been established for systems such as Mg–Al–Zn[75] and Al–Cu–Mg–Si[76], allowing systematic evaluation of the effects of alloying elements and secondary phases on TC. Based on this approach, high-thermal-conductivity alloys with face-centered cubic (FCC) structures, including Al–Zn, Al–Mg, and Al–Zn–Mg series, have been successfully designed, providing a transferable CALPHAD paradigm for the rational design of multicomponent alloys with enhanced thermal performance[77].

Based on established relationships between reciprocal of thermal diffusivity (RTD) and temperature for pure components, solid solutions, and multiphase alloys, TC can be calculated within the "composition–temperature–second phase" space, thereby imparting greater physical significance to existing TC equations [Figure 7A]. Xie *et al.* and Li *et al.* successfully predicted the TC of Mg–Zn/Al–La/Ce alloys[54,78]. As shown in Figure 7B, the TC distribution of Mg–Al–La ternary alloys in different two-phase regions was calculated using the Mg–Al–La TC database. The results show that the TC of the alloys gradually decreases with increasing alloying element and second-phase content. In particular, compared with the second phase, the solid solubility of Al in Mg has a more pronounced effect on reducing TC [Figure 7C][78]. However, CALPHAD models generally lack explicit descriptions of electronic structure, phonon dynamics, and defect-induced scattering processes, making it difficult to probe d atomic-scale mechanisms and unravel the fundamental physical nature of TC regulation. In multicomponent alloy systems, TC within the CALPHAD framework is typically modeled through semi-empirical formulations that rely on expert-defined parameters. These parameters are commonly calibrated using limited experimental data, enabling CALPHAD to capture macroscopic composition–temperature trends.

With the development of electron-phonon coupling calculation tools based on DFT calculation methods [Figure 7D], it has become possible to indirectly calculate the TC of electrons and phonons by modeling scattering processes of heat carriers[79,81,82]. These approaches provide a mechanistic understanding of how atomic-scale interactions, lattice vibrations, and electronic states govern heat transport. It has been shown that DFT-calculated TCs of pure Mg, Al, and Zn in the 300-700 K temperature range are in excellent agreement with experimental measurements [Figure 7E], confirming the reliability and applicability of DFT for predicting such properties[79]. By comparing the effects of different solute elements, it was found that Mn dissolved in the Mg matrix resulted in the most pronounced reduction in TC, followed by Sn, Ag, and Zn[83]. This variation is primarily attributed to differences in lattice distortion and electron-phonon scattering induced by solute atoms, indicating that DFT calculations can quantitatively assess microscopic perturbations caused by alloying elements and provide a theoretical basis for solute selection in the design of high-thermal-conductivity Mg alloys. Based on DFT calculations and the Cahill model, the minimum TCs of pure $Mg_{17}Al_{12}$ and M-doped (M = Ga, In, Ge, Sn, Pb) $Mg_{17}Al_{12}$ compounds along the [100], [110], and [111] directions were evaluated. As illustrated in Figure 7F, both pure $Mg_{17}Al_{12}$ and doped systems exhibit enhanced thermal transport along the [111] direction[80]. Although DFT can accurately capture microscopic mechanisms, it struggles to efficiently explore the high-dimensional "composition-processing-performance" space.

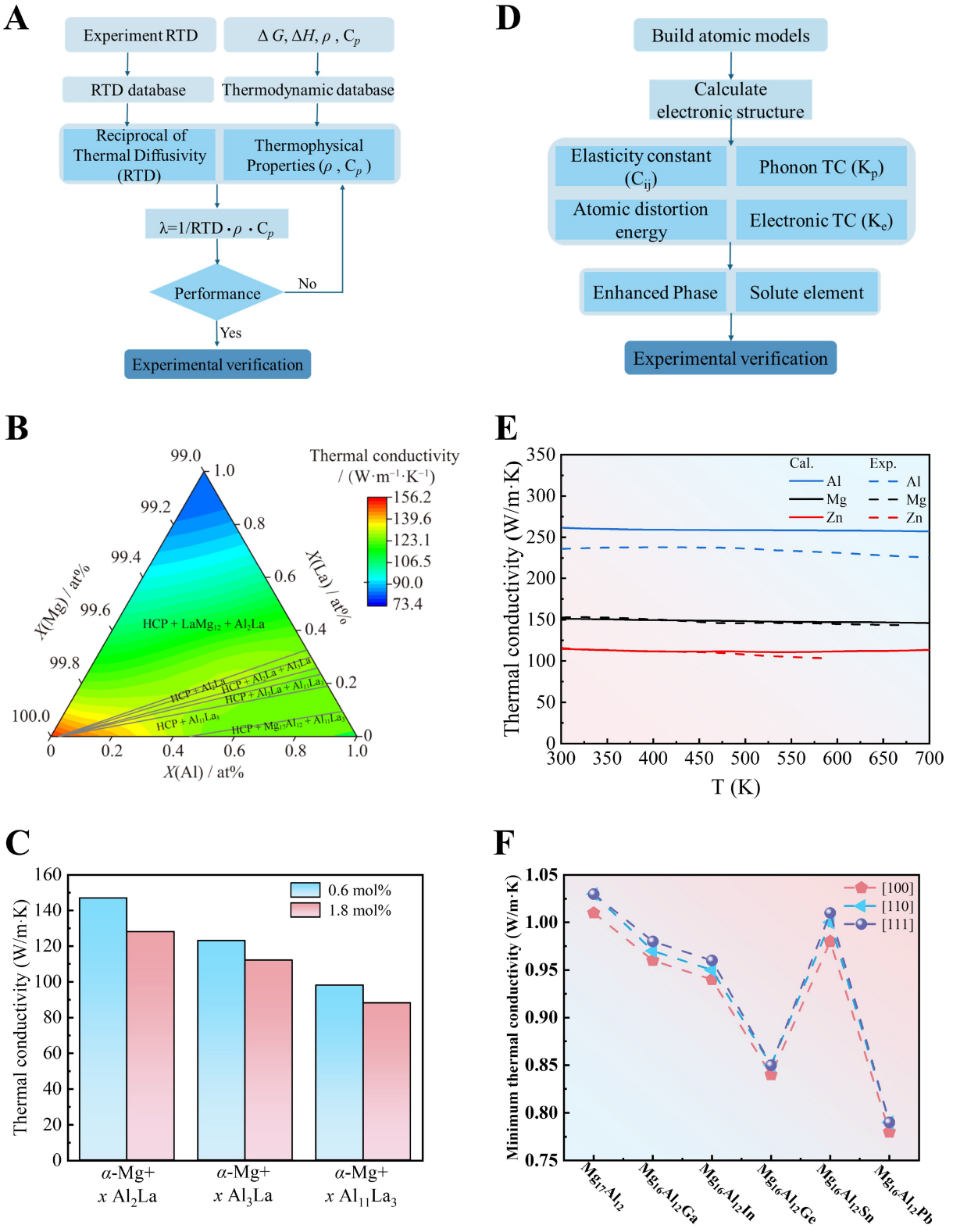

Figure 7. CALPHAD and DFT design TC alloys. (A) CALPHAD method alloy design procedure; (B) CALPHAD-predicted TC of Mg–Al–La alloys; (C) TC of alloys with varying second-phase contents at room temperature. (B and C) adapted from Ref.[78]. Copyright 2024, University of Science and Technology Beijing; (D) DFT method alloy design procedure; (E) Comparisons of calculated *vs.* experimental total TCs of Al, Mg, Zn with temperature. Adapted from Ref.[79]. Copyright 2021, Chinese Academy of Sciences; (F) The minimum TCs of pure $Mg_{17}Al_{12}$ and M-doped (M = Ga, In, Ge, Sn, Pb) $Mg_{17}Al_{12}$ compounds along the [100], [110], and [111] directions. Adapted from Ref.[80]. Copyright 2022, John Wiley and Sons. CALPHAD: CALculation of PHAse Diagrams; DFT: density functional theory; TC: thermal conductivity; RTD: reciprocal of thermal diffusivity.

ML can integrate thermodynamic data from CALPHAD, atomic-scale parameters from DFT calculations, and experimentally measured performance data, thereby enhancing model predictive performance through multi-source heterogeneous data fusion[84-86]. Furthermore, by leveraging its ability to handle high-dimensional inputs and capture complex nonlinear correlations, ML enables rapid exploration of composition–processing–structure–property relationships that are inaccessible using conventional approaches. This capability not only accelerates the prediction of alloy performance but also facilitates the identification of optimal composition–processing combinations, supporting a data-driven and mechanism-informed alloy design strategy. A novel ML approach integrated with multiscale computations has been proposed for predicting the TC of multicomponent Mg alloys[87]. A multiscale feature set was constructed, comprising elemental properties, thermodynamic parameters, and electronic structure descriptors, covering 1,139 as-cast Mg alloys. By integrating these key features, the Extreme gradient boosting (XGBoost) model achieved significantly improved prediction accuracy for the TC of low-component Mg alloys. Furthermore, the introduction of L1 (Lasso) and L2 (Ridge) regularization enhanced the extrapolation capability of the ML model for novel quaternary and higher-order systems. A physically informed symbolic regression method was also proposed to analyze the relative importance of different features affecting conductivity, while quantifying the contribution of each functional term through equation decomposition[88]. Nevertheless, the effectiveness of ML-based alloy design remains strongly constrained by data scarcity, incompleteness, and heterogeneity, particularly for multi-objective properties that are difficult or costly to measure. In this context, the systematic incorporation of materials expert knowledge - such as phase stability criteria and physically meaningful descriptors - has become essential for guiding data construction, constraining model predictions, and enhancing both the reliability and interpretability of ML-driven alloy design.

MULTI-OBJECTIVE DESIGN OF Mg/Al ALLOYS WITH STRENGTH AND TC

CALPHAD and DFT approaches for multi-objective alloy design

In the design of multi-objective alloys, the CALPHAD method is primarily employed to transform multiple property requirements into thermodynamically quantifiable phase characteristics (such as phase type, morphology, fraction, and solidification path)[89-91]. By coupling assessed thermodynamic/kinetic databases with equilibrium and Scheil calculations, CALPHAD provides a composition-process-phase map that supports rapid composition screening and constraint setting (e.g., suppression of deleterious intermetallic phases). Guided by these predictions, candidate Mg/Al alloys are optimized via iterative computational–experimental validation, where measured phase and microstructure data are fed back to refine the design space and accelerate multi-objective development. In a previous study, the CALPHAD method was employed to calculate the phase constitution [Figure 8A] and solidification path [Figure 8B] of an Al–Fe–Ni alloy, yielding a UTS of 131.2 ± 2.5 MPa, an elongation (EL) of 20.2% ± 3.6% [Figure 8C], and an electrical conductivity of 52.0% ± 0.1% of the International Annealed Copper Standard (IACS)[49]. Similarly, this method was applied to quantitatively optimize the Y content in both the long-period stacking ordered (LPSO) phase and the α-Mg matrix. By leveraging CALPHAD-guided phase diagram calculations and solidification simulations, the strengthening effect of the LPSO phase and the toughening contribution of the Y-enriched α-Mg matrix can be quantitatively balanced, enabling the design of Mg–Y–Al alloys with a desirable synergy of high strength and high ductility[92]. CALPHAD predictions of secondary-phase types and volume fractions, together with composition-dependent Zn solubility in the α-Mg matrix, provide an efficient route to tailoring microstructural partitioning, thereby achieving the concurrent improvement of alloy strength and TC[54].

The DFT method, starting from the atomic–electronic scale, is employed to accurately calculate the electronic structure, interatomic interactions, and microscopic structural parameters of alloys[93-96]. In this way, the structure–property relationships can be elucidated, enabling targeted regulation of strengthening

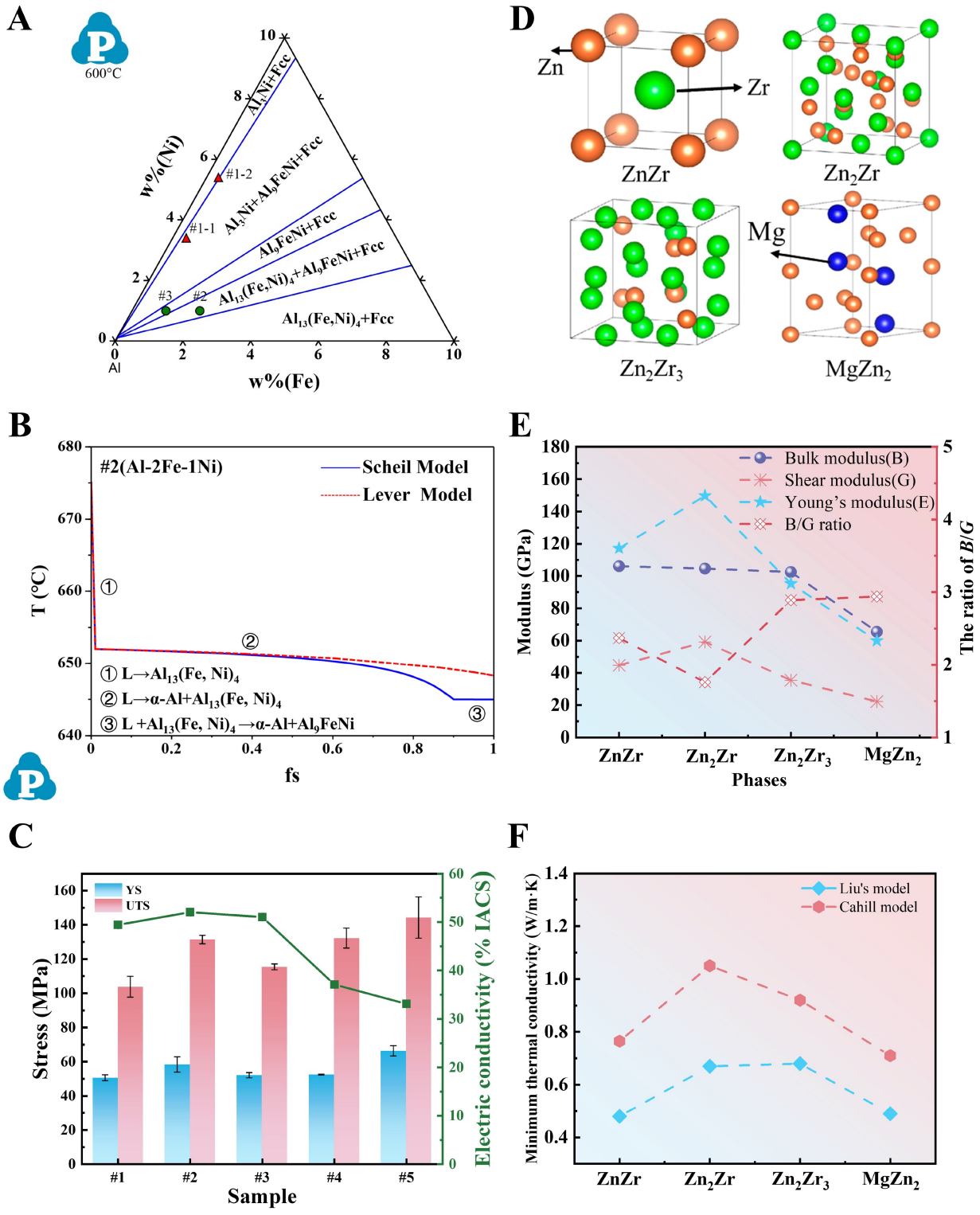

Figure 8. CALPHAD and DFT-guided design of strength and TC alloys. (A) Isothermal section of the Al–Fe–Ni system at 600 °C; (B) Solidification paths predicted by different models; (C) Property variations. (A-C) adapted from Ref.[49]. Copyright 2024, Elsevier; (D) Crystal structures of strengthening phases in the Mg-Zn-Zr System; (E) Mechanical properties; (F) Minimum thermal conductivities of four intermetallic compounds evaluated using the Cahill equation and Liu's model. (D-F) adapted from Ref.[98]. Copyright 2018, MDPI. CALPHAD: CALculation of PHAse Diagrams; DFT: density functional theory; TC: thermal conductivity; FCC: face-centered cubic; YS: yield strength; UTS: ultimate tensile strength; IACS: International Annealed Copper Standard.

mechanisms and electron transport behavior, thereby achieving synergistic optimization of strength and TC. First, phase stability is evaluated through phonon dispersion and binding energy calculations to screen potential strengthening phases. Subsequently, elastic modulus and hardness are calculated to elucidate the mechanisms responsible for high strength. Finally, Debye temperature and TC are assessed to evaluate heat conduction performance, and electronic structure analysis is employed to clarify metallic conduction characteristics[97]. For example, Wang *et al.* employed first-principles calculations to evaluate the mechanical properties and minimum TCs of strengthening phases (ZnZr, Zn_2Zr, Zn_2Zr_3, and $MgZn_2$) in Mg-Zn-Zr alloys[98]. The crystal structures of these four intermetallic compounds are illustrated in Figure 8D. As shown in Figure 8E, the bulk modulus (B), shear modulus (G), and Young's modulus (E) of Zn-Zr intermetallic compounds are higher than those of $MgZn_2$, indicating a more pronounced strengthening effect. Furthermore, the minimum TCs of the four intermetallic compounds are 0.48, 0.67, 0.68, and 0.49 W/m·K [Figure 8F], respectively. This suggests that the precipitation of Zn atoms from the α-Mg matrix to form binary Zn-Zr phases can enhance the overall TC of Mg-Zn-Zr alloys.

Both CALPHAD and DFT methods exhibit evident limitations in multi-objective alloy design. CALPHAD is highly dependent on existing thermodynamic databases, and its predictive capability for unknown systems or metastable phases remains limited. Moreover, it cannot quantitatively capture critical microstructural features such as phase morphology and interfacial structure, and only provides indirect inference through solidification pathways, rather than directly addressing factors governing electron scattering and strengthening effects. Although DFT can elucidate strengthening mechanisms and thermal transport behavior at the atomic–electronic scale, its applicability is restricted by computational scale. It cannot simulate realistic microstructural features such as multiphase coexistence and grain boundaries, and is typically limited to predicting the properties of individual phases. As a result, it fails to reflect the comprehensive impact of multiphase synergy on achieving high strength and high TC.

ML for multi-objective alloy design

ML offers an effective pathway to bridge the gap between CALPHAD and DFT in multi-objective alloy design. By integrating CALPHAD-derived thermodynamic descriptors, DFT-based atomic-scale features, and experimentally measured microstructure–property data, ML can learn nonlinear composition–process–structure–property mappings and capture complex effects that are difficult to model explicitly. More importantly, ML provides a practical computational strategy to formulate and solve multi-objective optimization problems in high-dimensional search spaces, enabling efficient screening beyond database coverage or first-principles calculations. To address the complexity of multi-objective alloy design, three distinct ML strategies are commonly employed [Figure 9]. The first strategy simplifies the problem by converting multiple objectives into a single scalar value. The second strategy constructs independent predictive models for various properties within a unified virtual design space. The third strategy leverages genetic algorithms to perform Pareto-based optimization, identifying the optimal trade-offs among competing alloy properties.

Strategy 1 maps multiple objectives into a single objective and then employs a single-objective optimization approach to identify the optimal solution, thereby achieving simultaneous optimization of multiple performance metrics[99-101]. This weighted single-objective transformation is selected mainly for its high computational efficiency in integrating conflicting targets - such as strength *vs.* TC - into a unified scalar. However, although this strategy is most applicable when performance priorities are predefined, the weighting process inevitably introduces subjectivity. In the performance optimization of Mg alloys, a method combining the light gradient boosting machine (LightGBM, LGBM) model with the multi-objective genetic algorithm, non-dominated sorting genetic algorithm III (NSGA-III), was proposed. After obtaining the optimal Pareto front, the mechanical properties of the three objectives were converted into a single scalar

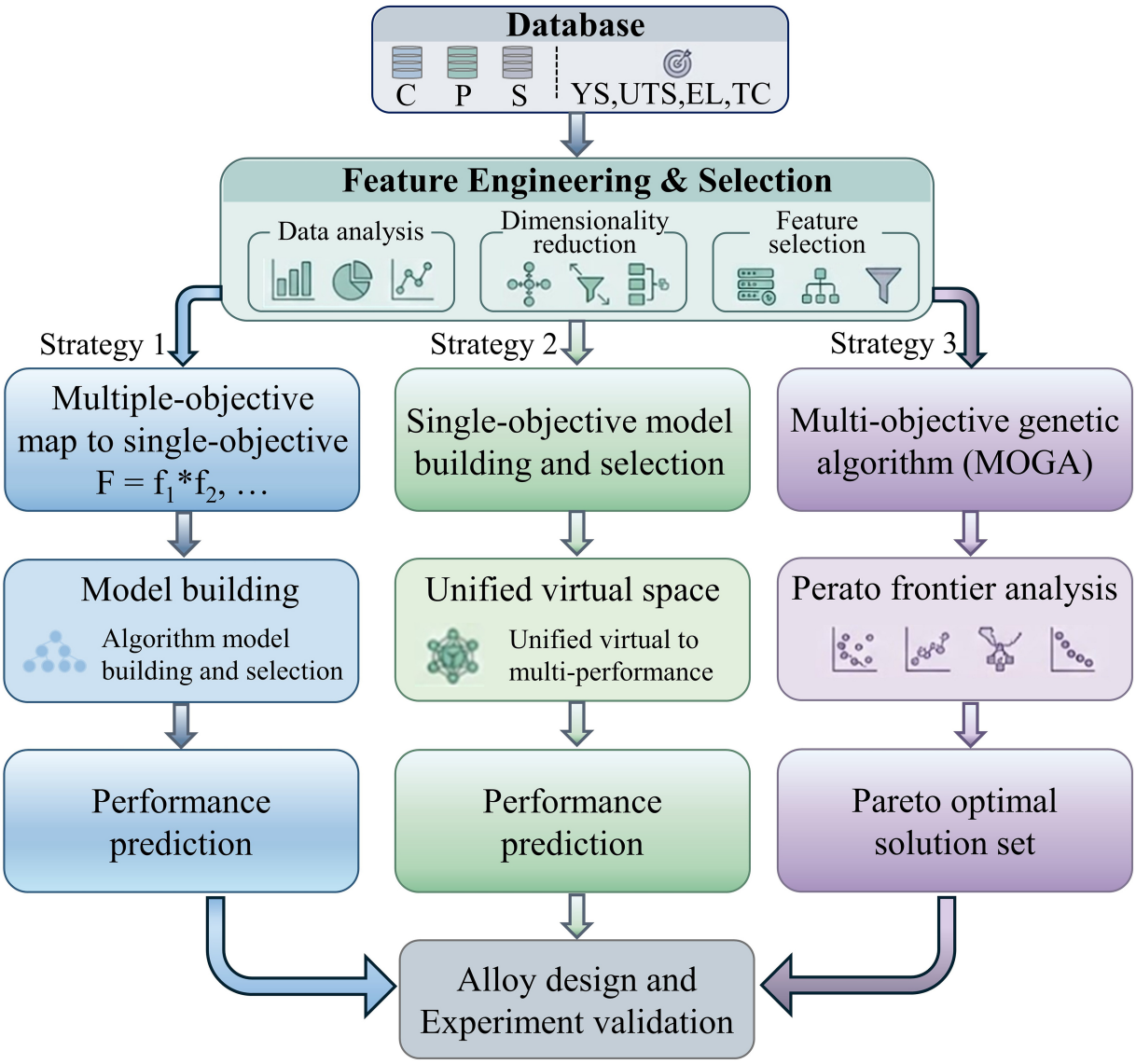

Figure 9. Three ML strategies for multi-objective alloy design. ML: Machine learning; YS: yield strength; UTS: ultimate tensile strength; EL: elongation; TC: thermal conductivity.

value (comprehensive performance)[102]. By constructing a high-quality database of alloy compositions, processing parameters, and calculated alloy descriptors, and applying feature selection techniques, high model accuracy was achieved. This approach successfully generated a three-dimensional Pareto front [Figure 10] and ranked candidate alloys using a comprehensive performance index, leading to the identification of optimal compositions with superior properties compared to the original dataset.

Specifically, Strategy 2 involves independent property modeling within a unified virtual space, an approach designed to maximize the utility of non-aligned datasets. By enabling independent modeling of individual properties - such as strength or TC - this strategy effectively resolves the common challenge of incomplete multi-property data. In practice, independent ML predictive models are first established for strength and TC, respectively. Subsequently, optimization algorithms are employed to explore the design space and identify two distinct sets of candidate alloys: those with optimal strength and those with optimal TC. By comparing these two sets of solutions, researchers can pinpoint common alloy formulations that simultaneously satisfy both requirements, thereby achieving a balance between conflicting properties[8]. This strategy has been

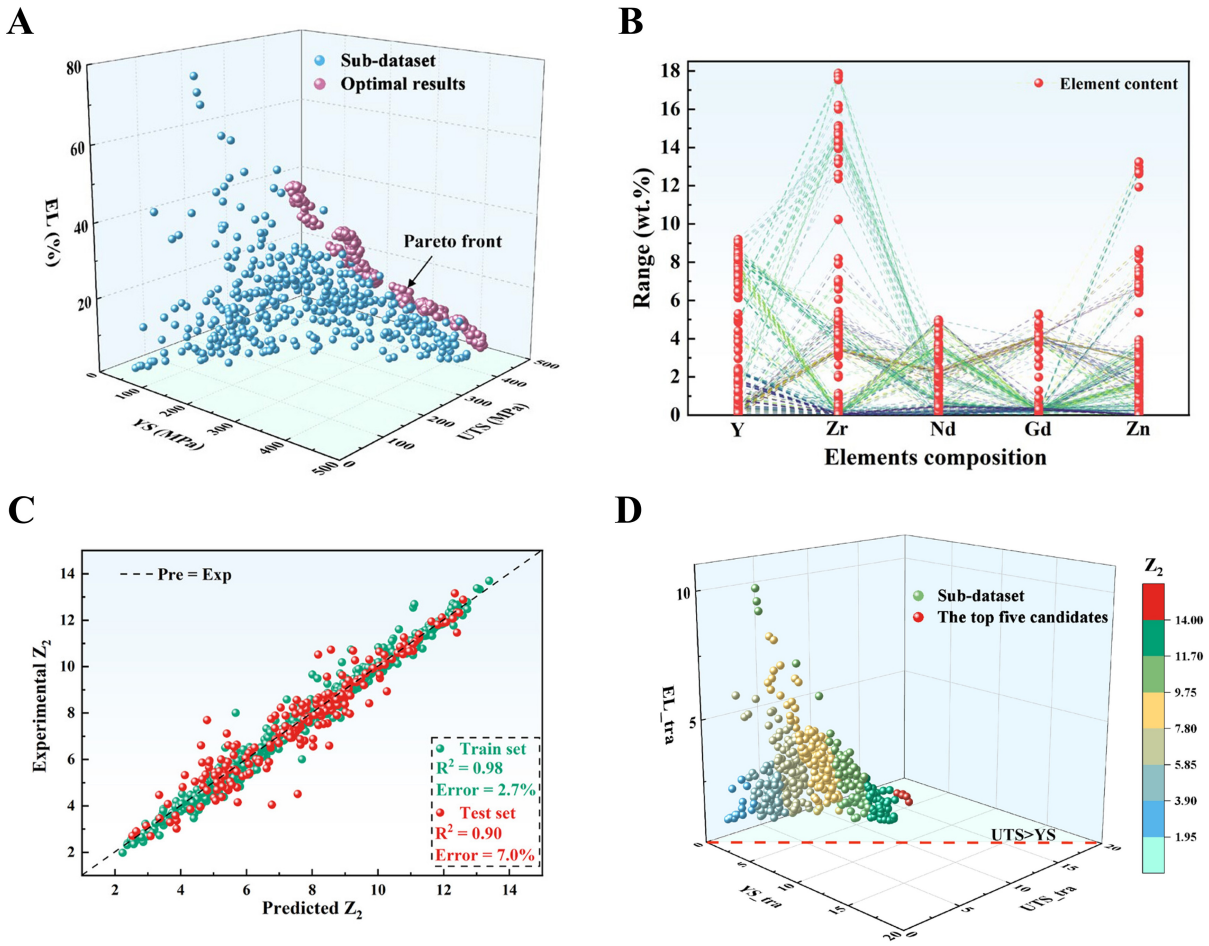

Figure 10. Mapping multi-objectives to a single objective. (A) Mechanical properties of the sub-dataset and the Pareto front; (B) Compositions of Mg alloys on the Pareto front; (C) Conversion into a single-objective performance prediction model; (D) Top five candidate alloys. (A-D) adapted from Ref.[102]. Copyright 2024, John Wiley & Sons Inc. EL: Elongation; YS: yield strength; UTS: ultimate tensile strength.

effectively applied in the design of high-strength and high-thermal-conductivity Al alloys, where a dataset of 277 entries was utilized to integrate property-specific information. XGBoost and support vector machine (SVM) methods were employed to establish predictive models for TC and UTS, respectively, as illustrated in Figure 11A. Physicochemical features were introduced and processed through feature engineering using the Lasso method and the Gini impurity criterion. Based on predictions for 800 virtual alloy samples [Figure 11B], a candidate composition (Al-2.64Si-0.43Mg-0.10Zn-0.03Cu) satisfying the target performance criteria was identified. The predictive results were further validated experimentally, confirming the reliability of the ML models [Figure 11C][8].

The Pareto optimization method has emerged as a more suitable approach for complex alloy design, as it avoids the need to transform multiple objectives into a single scalar value. Instead, Strategy 3 identifies non-dominated solutions to construct a Pareto front, thereby yielding an optimal solution set[103-106]. This model is specifically employed to explore the non-dominated solution set without requiring a priori weighting. By constructing a diverse decision space, it facilitates the integration of expert domain knowledge, enabling more nuanced trade-offs between mechanical reinforcement and thermal efficiency. For the synergistic optimization of porosity, hardness, and compressive strength in Al-Si-Mg nanocomposites, artificial neural networks have been used as fitness functions within the NSGA-II framework to perform

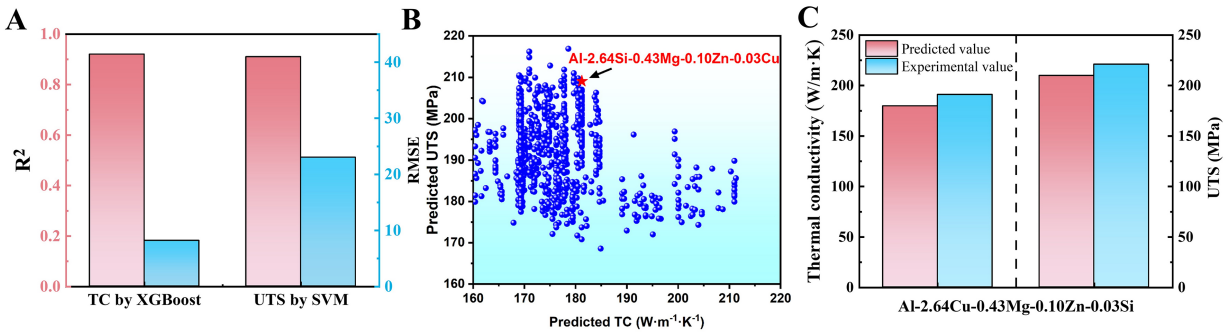

Figure 11. Single-objective models identify common optimal solutions within a shared virtual space. (A) Single-objective models; (B) Predicted TC and UTS values of 800 virtual samples generated by two models; (C) Comparison between predicted and experimental values. (A-C) adapted from Ref.[8]. Copyright 2024, OAE Publishing Inc. TC: Thermal conductivity; UTS: ultimate tensile strength; XGBoost: extreme gradient boosting; SVM: support vector machine; RMSE: root mean square error.

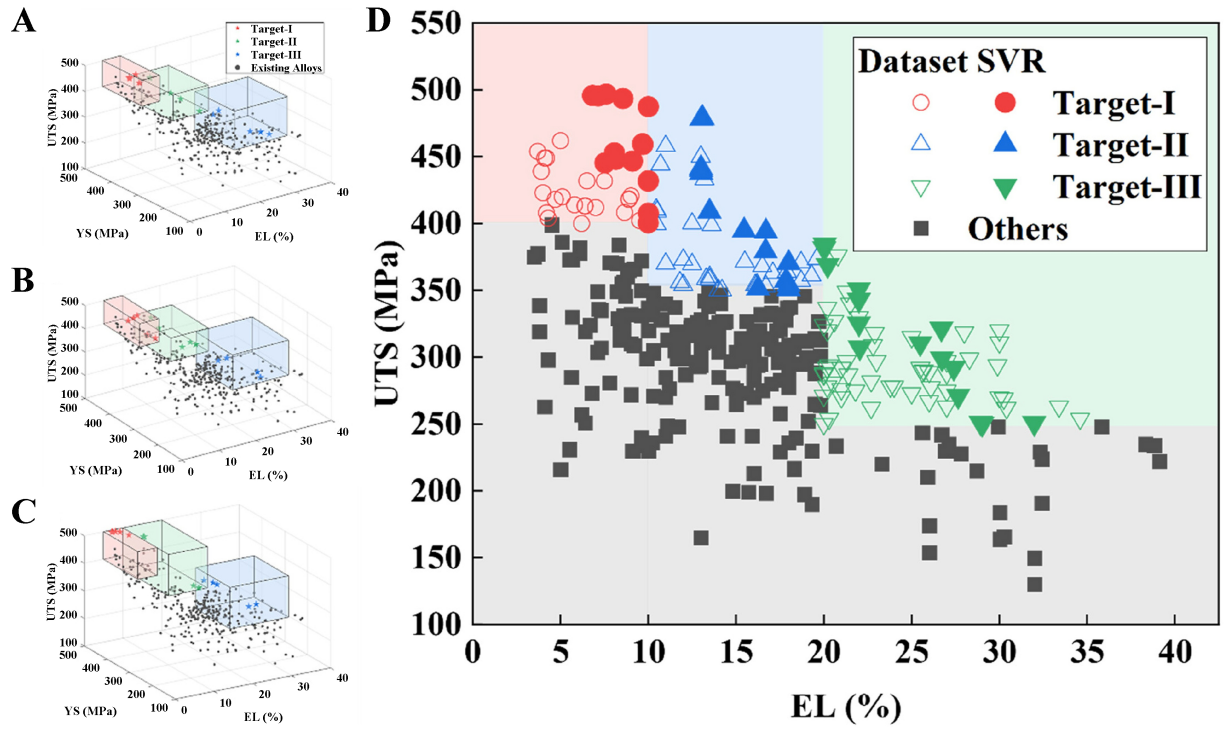

Figure 12. Comparison of YS, UTS, and EL values between triple-objective Pareto-optimal solutions and existing Mg alloys in the dataset, grouped by alloy systems: (A) Mg-Ca-Zn-Mn, (B) Mg-Al-Ca-Zn-Mn, and (C) Mg-Al-Ca-Zn-Mn-Sn alloys; (D) Strength–ductility map of datasets and design solutions. (A-D) adapted from Ref.[108]. Copyright 2024, John Wiley & Sons Inc. YS: Yield strength; UTS: ultimate tensile strength; EL: elongation; SVR: support vector regression.

multi-objective optimization of these target properties[107]. By integrating a support vector regression (SVR) model with a multi-objective genetic algorithm, Li *et al.* achieved three-objective optimization of the mechanical properties of extruded Mg alloys [Figure 12]. Specifically, five Pareto-optimal solutions were selected for each property. The proposed candidates were grouped by alloy system (Mg-Ca-Zn-Mn, Mg-Al-Ca-Zn-Mn, and Mg-Al-Ca-Zn-Mn-Sn) and systematically compared against the YS, UTS, and EL values of existing Mg alloys in the dataset. As shown in the UTS-EL relationship in Figure 12D, the designed optimization schemes substantially outperform the existing alloys in terms of overall mechanical performance[108].

These three strategies represent complementary paradigms for multi-objective alloy design, differing in their assumptions regarding data availability, optimization flexibility, and the degree of human intervention required. Weighted single-objective transformation offers computational efficiency when performance priorities are clearly defined, while independent property modeling provides a practical solution to data incompleteness by decoupling heterogeneous property datasets. Pareto-based optimization, in contrast, enables a more comprehensive exploration of the trade-off landscape and preserves solution diversity without imposing subjective weighting. Crucially, regardless of the optimization strategy employed, the effective incorporation of materials expert knowledge remains essential. Domain knowledge can be systematically integrated to constrain the design space, screen out non-physical or non-processable solutions, and guide the final selection of candidate alloys from the Pareto front based on metallurgical feasibility, phase stability, and processing considerations. By combining algorithmic optimization with expert-informed decision making, these strategies collectively enable a transition from purely data-driven optimization toward mechanism-aware, application-oriented multi-objective alloy design.

Potential and challenges of ML in multi-objective alloy design

Advances in materials genome engineering and high-throughput computing highlight the growing potential of ML for multi-objective alloy design[109,110]. ML can extract underlying patterns from complex CPSP relationships through large-scale data mining and pattern recognition, thereby providing new approaches for the simultaneous optimization of multiple properties such as YS, EL, and TC[111]. ML models can markedly accelerate alloy design by generating Pareto front solutions in multi-dimensional performance spaces, enabling balanced optimization of competing properties such as strength–ductility and mechanical–thermal performance. Meanwhile, interpretable methods such as SHapley Additive exPlanations (SHAP) and feature importance analysis elucidate key alloying elements and their interactions, offering theoretical guidance for experimental design.

Despite the potential of ML in alloy design, several challenges remain. Data scarcity and heterogeneity constrain model generalization, particularly due to the limited availability of multi-property datasets, which undermines predictive accuracy and reliability. To address these issues, domain knowledge is first incorporated into feature engineering by integrating physically meaningful descriptors (e.g., atomic radius and electronegativity as intrinsic elemental features). In addition, datasets can be constructed by combining experimental and simulated data through multi-scale computations such as DFT and CALPHAD. Second, dimensionality reduction techniques such as principal component analysis (PCA), along with feature importance analysis, are used to extract low-dimensional and informative representations. Finally, active learning and multi-objective optimization algorithms are employed to iteratively guide alloy design, enabling adaptive recommendation of optimal composition-process combinations and efficient exploration of the global multi-objective performance space.

The lack of interpretability remains a challenge, as most optimization outcomes still rely on black-box models that provide limited guidance for alloy design. On the one hand, techniques such as physics-informed neural networks (PINNs) embed known physical equations (e.g., YS formulas, thermodynamic constraints) as prior knowledge into the training process, ensuring that model predictions maintain physical consistency. On the other hand, interpretability tools such as SHAP are employed to explain the decision logic of the model, thereby uncovering complex nonlinear coupling relationships among composition-processing-performance variables. Crucially, these SHAP-derived insights facilitate scientific discovery. When interpreted through the lens of domain expertise, they enable researchers to decode underlying physical mechanisms - such as the synergistic effects between alloying elements and thermal processing parameters - that govern material behavior, ultimately transforming raw correlations into actionable design principles for technological innovation. However, the computational complexity of

multi-objective optimization is often high, raising the need to improve efficiency while maintaining both solution diversity and accuracy. Furthermore, integrating ML predictions with experimental validation and physical modeling to establish a "data–model–experiment" closed loop represents a critical direction for future development in this field.

Moreover, the systematic integration of materials domain knowledge into ML frameworks represents a key strategy for improving model robustness and ensuring the practical feasibility of multi-objective alloy design. In contrast to purely data-driven approaches, expert knowledge can guide the learning process across multiple stages, including data construction, feature engineering, and model constraint formulation. At the data level, materials knowledge - such as phase diagram information, strengthening mechanisms, and thermal transport mechanisms - can be leveraged to curate and annotate experimental datasets, thereby excluding thermodynamically or process-infeasible composition regions and effectively reducing the search space. At the feature level, incorporating physically informed descriptors closely associated with strengthening, TC, and plastic deformation mechanisms (e.g., solid-solution strengthening parameters, precipitate volume fractions, and electronic structure–related descriptors) enables the model to better capture the underlying drivers of property evolution. At the model and optimization level, domain-informed constraints reflecting metallurgical heuristics and process feasibility boundaries (such as solubility limits of alloying elements, phase stability criteria, and heat treatment windows) can be explicitly embedded, preventing the identification of solutions that are optimal in a mathematical sense but impractical for experimental realization. By coupling the efficient exploration capabilities of ML with expert-driven mechanistic insights, a transition from correlation-based prediction toward mechanism-informed alloy design can be achieved, substantially enhancing the reliability, interpretability, and real-world applicability of multi-objective design outcomes.

CONCLUSION AND OUTLOOK

The design of high-strength and high-thermal-conductivity Mg/Al alloys has transitioned from empirical discovery to computational materials engineering. This review bridges physical metallurgy and modern informatics strategies. The design concept is to precipitate solute atoms from the matrix, thereby restoring lattice integrity to facilitate electron transport, while simultaneously enhancing mechanical strength through the introduction of a second phase. This approach provides a viable pathway for mitigating the inherent trade-off between strength and electrical conductivity. We systematically analyze the computational toolkit driving this paradigm shift: CALPHAD delineates thermodynamic boundaries, DFT elucidates intrinsic transport physics, and ML accelerates the exploration of high-dimensional design spaces. While single-objective methods have laid the foundation, our review highlights that Multi-Objective Optimization frameworks represent a more robust strategy. These approaches utilize physics-based parameters as high-fidelity descriptors, enabling efficient mapping of the Pareto frontier to balance conflicting properties.

Despite significant progress, several critical frontiers remain for next-generation alloy design. Foremost among these is the challenge of data scarcity and high-dimensional feature representation. High-quality datasets for TC are rare and heterogeneous. In addition, the high dimensionality of composition and processing spaces renders purely data-driven approaches inefficient. Future work would likely benefit from Transfer Learning (transferring knowledge from data-rich Al systems to Mg systems) and active learning loops, which are expected to maximize information gain from limited experiments. Concurrently, expert involvement in data curation, feature validation, and physical consistency checking remains indispensable, serving as a critical safeguard for data reliability and model robustness.

A second major frontier involves enhancing physical consistency through explainable AI. Black-box models face limitations in accurately reflecting rigorous physical metallurgy principles. To enhance generalizability and build confidence in predictive models, the adoption of explainable AI methods, such as SHAP, is

essential. By integrating algorithmic approaches with expert domain knowledge, the patterns identified by AI can be interpreted from a domain-informed perspective and translated into meaningful scientific insights and technological innovations, thereby ensuring that model outputs remain consistent with established metallurgical principles.

Finally, a pivotal objective for future research is the paradigm shift from discriminative screening and forward prediction to generative inverse design. Emerging generative AI techniques, such as GANs and VAEs, hold significant potential for effectively navigating the continuous latent space of material design. However, the future development of these technologies depends not only on the deployment of complex algorithms, but more importantly on the establishment of large-scale, high-fidelity datasets grounded in physical principles and curated with expert guidance. Such efforts are essential to ensure that AI-generated insights align with scientific reality.

DECLARATIONS

Authors' contributions

Made substantial contributions to the conception and design of this review, as well as writing and editing: Chen, Y.; Chen, H.; Luo, Q.

Made substantial contributions to literature collation, figure preparation, and writing: Chen, Y.; Hu, L.; Tang, K.; Liu, B.; Zhang, Y.; Hu, B.

Performed data acquisition and provided administrative, technical, and material support: Luo, Q.; Li, Q.

Availability of data and materials

Not applicable.

AI and AI-assisted tools statement

During the preparation of this manuscript, the AI tool Google Gemini (Version Gemini 3.1 Pro) was used solely for language editing. The tool did not influence the study design, data collection, analysis, interpretation, or the scientific content of the work. All authors take full responsibility for the accuracy, integrity, and final content of the manuscript.

Financial support and sponsorship

This research was funded by the National Natural Science Foundation of China (52422407, 52371010, and U2102212) and the Chongqing Science and Technology Commission, China (CSTC2024YCJH-BGZXM0041).

Conflicts of interest

Li, Q. serves as an Associate Editor of *Journal of Materials Informatics* and as a Guest Editor for the Special Issue entitled "Machine Learning/AI-Assisted Development of High-Performance Alloys". He is not involved in any stage of the editorial process, notably including reviewer selection, manuscript handling, or decision making. The other authors declared that there are no conflicts of interest.

Ethical approval and consent to participate

Not applicable.

Consent for publication

Not applicable.

REFERENCES

1. Kawamura, Y.; Ougi, K.; Inoue, S.; et al. Advanced Mg–Al–Ca alloys with combined properties of high thermal conductivity, high mechanical strength and non-flammability. *Mater. Trans.* **2022**, *63*, 118-27. DOI

2. Hou, J.; Li, D.; Liu, Z.; et al. Structure-function integrated magnesium alloys and their composites. *J. Magnes. Alloys.* **2023**, *11*, 3511-44. DOI
3. Chen, H.; Wen, H.; Sun, J.; et al. Quantitative exploration of aging–precipitate–property relationship in Mg-Gd alloys. *J. Mater. Sci. Technol.* **2026**, *245*, 221-6. DOI
4. Tan, J.; Zhang, Y. Thermal conductive polymer composites: recent progress and applications. *Molecules* **2024**, *29*, 3572. DOI PubMed PMC
5. Anis, A.; Elnour, A. Y.; Alam, M. A.; Al-Zahrani, S. M.; AlFayez, F.; Bashir, Z. Aluminum-filled amorphous-PET, a composite showing simultaneous increase in modulus and impact resistance. *Polymers* **2020**, *12*, 2038. DOI PubMed PMC
6. Chen, H.; Sun, J.; Yang, S.; et al. Thermodynamics and kinetics of isothermal precipitation in magnesium alloys. *Mater. Genome. Eng. Adv.* **2025**, *3*, e86. DOI
7. Fan, J.; Yang, Q.; Lv, S.; et al. Synergetic tensile properties and thermal conductivity of high-pressure die casting Mg-Al-RE alloys controlling by various Al and La additions. *J. Alloys. Compd.* **2025**, *1032*, 181121. DOI
8. Lu, Z.; Kapoor, I.; Li, Y.; Liu, Y.; Zeng, X.; Wang, L. Machine learning driven design of high-performance Al alloys. *J. Mater. Inf.* **2024**, *4*, 19. DOI
9. Dong, Q.; Zhang, Y.; Wang, J.; Huang, L.; Nagaumi, H. Enhanced strength-conductivity trade-off in Al-Mg-Si alloys with optimized Mg/Si ratio. *J. Alloys. Compd.* **2024**, *970*, 172682. DOI
10. Lv, H.; Tan, J.; Geng, T.; et al. Advances in high-strength and high-thermal conductivity cast magnesium alloys: strategies for property optimization. *J. Alloys. Compd.* **2025**, *1029*, 180843. DOI
11. Shang, Q.; Tan, J.; Lv, H.; et al. Breaking the trade-off between thermal conductivity and strength of magnesium alloys: mechanisms and strategies. *Curr. Opin. Solid. State. Mater. Sci.* **2025**, *37*, 101230. DOI
12. Lv, H.; Shang, Q.; Tan, J.; et al. Breaking the trade-off between mechanical properties and thermal conductivity of magnesium alloys via regulating the partial Gibbs energy of alloying elements. *Acta. Mater.* **2025**, *289*, 120894. DOI
13. Vasudevan, R. K.; Choudhary, K.; Mehta, A.; et al. Materials science in the AI age: high-throughput library generation, machine learning and a pathway from correlations to the underpinning physics. *MRS. Commun.* **2019**, *9*, 821-38. DOI PubMed PMC
14. Cheng, Y.; Wang, L.; Yang, C.; et al. A brief review of machine learning-assisted Mg alloy design, processing, and property predictions. *J. Mater. Res. Technol.* **2024**, *30*, 8108-27. DOI
15. Rahman, A.; Hossain, M. S.; Siddique, A. Review: machine learning approaches for diverse alloy systems. *J. Mater. Sci.* **2025**, *60*, 12189-221. DOI
16. Wang, C.; Fu, H.; Jiang, L.; Xue, D.; Xie, J. A property-oriented design strategy for high performance copper alloys via machine learning. *npj. Comput. Mater.* **2019**, *5*, 227. DOI
17. Zhang, H.; Fu, H.; He, X.; et al. Dramatically enhanced combination of ultimate tensile strength and electric conductivity of alloys via machine learning screening. *Acta. Mater.* **2020**, *200*, 803-10. DOI
18. Ren, D.; Wang, C.; Wei, X.; Lai, Q.; Xu, W. Building a quantitative composition-microstructure-property relationship of dual-phase steels via multimodal data mining. *Acta. Mater.* **2023**, *252*, 118954. DOI
19. Ma, J.; Zhang, W.; Han, Z.; Xu, Q.; Zhao, H. An explainable deep learning model based on multi-scale microstructure information for establishing composition–microstructure–property relationship of aluminum alloys. *Integr. Mater. Manuf. Innov.* **2024**, *13*, 827-42. DOI
20. Kocks, U. F.; Argon, A. S.; Ashby, M. F. *Thermodynamics and kinetics of slip*. Pergamon; 1975. pp. 141-5. https://books.google.com/books?id=1zukswEACAAJ. (accessed 2026-05-18).
21. Ryen, Ø.; Holmedal, B.; Nijs, O.; Nes, E.; Sjölander, E.; Ekström, H. Strengthening mechanisms in solid solution aluminum alloys. *Metall. Mater. Trans. A.* **2006**, *37*, 1999-2006. DOI
22. Rupert, T. J.; Trenkle, J. C.; Schuh, C. A. Enhanced solid solution effects on the strength of nanocrystalline alloys. *Acta. Mater.* **2011**, *59*, 1619-31. DOI
23. Mohri, T.; Suzuki, T. Solid solution hardening by impurities. In *Impurities in engineering materials*, 1st ed.; Routledge, 2017; pp. 259-99. https://www.taylorfrancis.com/chapters/edit/10.1201/9780203751190-9/solid-solution-hardening-impurities-tetsuo-mohri-tomoo-suzuki. (accessed 2026-05-18).
24. Suzuki, A.; Saddock, N.; Riester, L.; Lara-Curzio, E.; Jones, J.; Pollock, T. Effect of Sr additions on the microstructure and strength of a Mg-Al-Ca ternary alloy. *Metall. Mater. Trans. A.* **2007**, *38*, 420-7. DOI
25. Pan, F.; Yang, M.; Chen, X. A review on casting magnesium alloys: modification of commercial alloys and development of new Alloys. *J. Mater. Sci. Technol.* **2016**, *32*, 1211-21. DOI
26. Yang, Y.; Li, X. Influence of neodymium on high cycle fatigue behavior of die cast AZ91D magnesium alloy. *J. Rare. Earths.* **2010**, *28*, 456-60. DOI
27. Hall, E. O. The deformation and ageing of mild steel: III discussion of results. *Proc. Phys. Soc. B.* **1951**, *64*, 747-53. DOI

28. Liu, D.; Zhao, H.; Wang, L. Numerical investigation of grain refinement of magnesium alloys: effects of cooling rate. *J. Phys. Chem. Solids.* **2020**, *144*, 109486. DOI
29. Liang, G.; Ali, Y.; You, G.; Zhang, M. Effect of cooling rate on grain refinement of cast aluminium alloys. *Materialia* **2018**, *3*, 113-21. DOI
30. Wei, Y.; Wang, C.; You, J.; et al. Substantial grain refinement of Al-Mn-Si alloys mediated by collaborative effect of Al-5Ti-1B refiner and sub-rapid solidification. *J. Mater. Sci. Technol.* **2024**, *187*, 230-9. DOI
31. Yang, J.; Sui, Y.; Jiang, Y.; Li, P. Effect of Zr addition on the microstructure and mechanical properties of as-cast Al-Mg-Mn-Sc alloys. *Inter. Metalcast.* **2025**, *19*, 2881-92. DOI
32. Liu, Y.; Yu, J.; Wu, G.; et al. Grain refinement mechanism in gradient nanostructured Mg-Gd-Y-Zn-Zr alloy prepared by severe shear deformation. *Mater. Sci. Eng. A.* **2024**, *894*, 146207. DOI
33. Li, Y.; Wu, G.; Chen, A.; et al. Effects of Gd and Zr additions on the microstructures and high-temperature mechanical behavior of Mg–Gd–Y–Zr magnesium alloys in the product form of a large structural casting. *J. Mater. Res.* **2015**, *30*, 3461-73. DOI
34. Maghzi, M.; Mirzadeh, H.; Mahmudi, R. Grain refinement and improved mechanical properties of as-cast Mg-3Gd alloy by Zr addition. *J. Mater. Res. Technol.* **2025**, *35*, 2346-53. DOI
35. Cao, Y.; Wang, L.; Guo, E.; et al. Grain refinement and exceptional creep resistance achieved in an as-cast Mg–Y alloy with Al addition. *Mater. Sci. Eng. A.* **2024**, *901*, 146587. DOI
36. Yin, H.; Liu, Z.; Liu, X.; Fan, R.; Liu, Y.; Li, J. Effects of Al addition on the microstructure and mechanical properties of Mg–4Y alloys. *Mater. Sci. Technol.* **2017**, *33*, 2188-96. DOI
37. Dai, J.; Zhu, S.; Easton, M. A.; et al. Heat treatment, microstructure and mechanical properties of a Mg–Gd–Y alloy grain-refined by Al additions. *Mater. Sci. Eng. A.* **2013**, *576*, 298-305. DOI
38. Jiang, Z.; Meng, X.; Jiang, B.; et al. Grain refinement of Mg-3Y alloy using Mg-10Al2Y master alloy. *J. Rare. Earths.* **2021**, *39*, 881-8. DOI
39. Jia, Y.; Huang, H.; Fu, Y.; et al. An *in situ* investigation of the solute suppressed nucleation zone in an Al-15 wt% Cu alloy inoculated by Al-Ti-B. *Scr. Mater.* **2019**, *167*, 6-10. DOI
40. Zhang, C.; Liao, W.; Shan, Z.; Song, W.; Dong, X. Squeeze casting of 4032 aluminum alloy and the synergetic enhancement of strength and ductility via Al-Ti-Nb-B grain refiner. *Mater. Sci. Eng. A.* **2024**, *896*, 146233. DOI
41. Nie, J. Effects of precipitate shape and orientation on dispersion strengthening in magnesium alloys. *Scr. Mater.* **2003**, *48*, 1009-15. DOI
42. Nie, J. Precipitation and hardening in magnesium alloys. *Metall. Mater. Trans. A.* **2012**, *43*, 3891-939. DOI
43. Zhao, C.; Chen, X.; Wang, J.; et al. Strain hardening behavior in Mg–Al alloys at room temperature. *Adv. Eng. Mater.* **2019**, *21*, 1801062. DOI
44. Wang, A.; Sheng, Y. F.; Bao, H. Recent advances in thermal transport theory of metals. *Acta. Phys. Sin.* **2024**, *73*, 037201. DOI
45. Tong, Z.; Li, S.; Ruan, X.; Bao, H. Comprehensive first-principles analysis of phonon thermal conductivity and electron-phonon coupling in different metals. *Phys. Rev. B.* **2019**, *100*, 144306. DOI
46. Zeng, X.; Wang, J.; Ying, T.; Ding, W. Recent progress on thermal conductivity of magnesium and its alloys. *Acta. Metall. Sin.* **2022**, *58*, 400-11. DOI
47. Su, C.; Li, D.; Luo, A. A.; Ying, T.; Zeng, X. Effect of solute atoms and second phases on the thermal conductivity of Mg-RE alloys: a quantitative study. *J. Alloys. Compd.* **2018**, *747*, 431-7. DOI
48. Pan, H.; Pan, F.; Yang, R.; et al. Thermal and electrical conductivity of binary magnesium alloys. *J. Mater. Sci.* **2014**, *49*, 3107-24. DOI
49. Zhang, Y.; Luo, X.; Zhu, L.; et al. Design of non-heat-treatable Al-Fe-Ni alloys with high electrical conductivity and high strength via CALPHAD approach. *J. Alloys. Compd.* **2024**, *1009*, 176920. DOI
50. Zhang, A.; Li, Y. Effect of alloying elements on thermal conductivity of aluminum. *J. Mater. Res.* **2023**, *38*, 2049-58. DOI
51. Choi, S.; Cho, H.; Kumai, S. Effect of the precipitation of secondary phases on the thermal diffusivity and thermal conductivity of Al-4.5Cu alloy. *J. Alloys. Compd.* **2016**, *688*, 897-902. DOI
52. Zhong, L.; Wang, Y.; Gong, M.; Zheng, X.; Peng, J. Effects of precipitates and its interface on thermal conductivity of Mg–12Gd alloy during aging treatment. *Mater. Charact.* **2018**, *138*, 284-8. DOI
53. Yao, F.; Li, Z.; Hu, B.; Jiang, Z.; Zeng, X.; Li, D. Unveiling the interface between second phases and matrix on thermal conductivity of Mg alloys. *J. Mater. Res. Technol.* **2024**, *28*, 1824-33. DOI
54. Xie, T.; Shi, H.; Wang, H.; Luo, Q.; Li, Q.; Chou, K. Thermodynamic prediction of thermal diffusivity and thermal conductivity in Mg–Zn–La/Ce system. *J. Mater. Sci. Technol.* **2022**, *97*, 147-55. DOI
55. Dong, H.; Wen, B.; Melnik, R. Relative importance of grain boundaries and size effects in thermal conductivity of nanocrystalline materials. *Sci. Rep.* **2014**, *4*, 7037. DOI PubMed PMC
56. Rowe, D. M.; Shukla, V. S. The effect of phonon-grain boundary scattering on the lattice thermal conductivity and thermoelectric conversion efficiency of heavily doped fine-grained, hot-pressed silicon germanium alloy. *J. Appl. Phys.* **1981**, *52*, 7421-6. DOI

57. Tong, X.; You, G.; Ding, Y.; Xue, H.; Wang, Y.; Guo, W. Effect of grain size on low-temperature electrical resistivity and thermal conductivity of pure magnesium. *Mater. Lett.* **2018**, *229*, 261-4. DOI
58. Kogure, Y.; Hiki, Y. Effect of dislocations on low-temperature thermal conductivity and specific heat of copper-aluminum alloy crystals. *J. Phys. Soc. Jpn.* **1975**, *39*, 698-707. DOI
59. Povoden-Karadeniz, E.; Lang, P.; Warczok, P.; Falahati, A.; Jun, W.; Kozeschnik, E. CALPHAD modeling of metastable phases in the Al–Mg–Si system. *Calphad* **2013**, *43*, 94-104. DOI
60. Uzunoğlu, Y. Computational study of the effect of aluminum content on the thermodynamic properties and phase stabilityof Mg-Al-Zn alloys. *ACS* **2025**, *2*, 36-42. DOI
61. Otani, Y.; Saki, K.; Takata, N.; Suzuki, A.; Kobashi, M.; Kato, M. CALPHAD-aided design of high-strength Al-Si-Mg alloys for sufficient laser powder bed fusion processability. *J. Alloys. Compd.* **2024**, *977*, 173449. DOI
62. Lan, X.; Li, K.; Wang, F.; et al. Preparation of millimeter scale second phase particles in aluminum alloys and determination of their mechanical properties. *J. Alloys. Compd.* **2019**, *784*, 68-75. DOI
63. Wen, T.; Li, Z.; Wang, J.; et al. CALPHAD aided design of a crack-free Al-Mg-Si-Ti alloy with high strength: heterogeneous nucleation and eutectic filling during additive manufacturing. *Virtual. Phys. Prototyp.* **2024**, *19*, e2378930. DOI
64. Pius, K. K.; Ongwen, N. O.; Mageto, M.; Odari, V.; Gaitho, F. M. Mechanical properties of Al–Mg–Si alloys (6xxx Series): a DFT-based study. *Alloys* **2023**, *2*, 213-26. DOI
65. Wang, C.; Han, P.; Zhang, L.; Zhang, C.; Yan, X.; Xu, B. The strengthening effect of Al atoms into Mg–Al alloy: a first-principles study. *J. Alloys. Compd.* **2009**, *482*, 540-3. DOI
66. Su, H.; Zhang, C.; Wang, S.; et al. Local atomic ordering strategy for high strength Mg alloy design by first-principle calculations. *J. Alloys. Compd.* **2022**, *907*, 164491. DOI
67. Zhou, Y.; Tian, W.; Lv, H.; et al. Designing high-strength and high-ductility cast Mg–Zn–Al–Mn–Sn alloys via τ-$Mg_{32}(Al,Zn)_{49}$ phase tuning and twin boundary toughening optimisation. *Rare. Metals.* **2026**, *45*, e70057. DOI
68. Ai, S.; Fang, D.; Guo, Y.; Ye, J.; Lin, X. Machine learning-driven prediction of microstructure-mechanical property relationships in Mg-Al alloys. *J. Alloys. Compd.* **2025**, *1036*, 181995. DOI
69. Li, J.; Zhang, Y.; Cao, X.; et al. Accelerated discovery of high-strength aluminum alloys by machine learning. *Commun. Mater.* **2020**, *1*, 74. DOI
70. Liu, Y.; Wang, L.; Zhang, H.; et al. Accelerated development of high-strength magnesium alloys by machine learning. *Metall. Mater. Trans. A.* **2021**, *52*, 943-54. DOI
71. Zhu, G.; Du, X.; Sun, D. Machine learning accelerated design of magnesium alloys with high strength and high ductility. *Mater. Today. Commun.* **2025**, *44*, 111894. DOI
72. Zhu, L.; Luo, Q.; Chen, Q.; et al. Prediction of ultimate tensile strength of Al-Si alloys based on multimodal fusion learning. *Mater. Genome. Eng. Adv.* **2024**, *2*, e26. DOI
73. Su, C.; Li, D.; Luo, A. A.; Shi, R.; Zeng, X. Quantitative study of microstructure-dependent thermal conductivity in Mg-4Ce-xAl-0.5Mn alloys. *Metall. Mater. Trans. A.* **2019**, *50*, 1970-84. DOI
74. Avraham, S.; Maoz, Y.; Bamberger, M. Application of the CALPHAD approach to Mg-alloys design. *Calphad* **2007**, *31*, 515-21. DOI
75. Huang, L.; Liu, S.; Du, Y.; Zhang, C. Thermal conductivity of the Mg–Al–Zn alloys: experimental measurement and CALPHAD modeling. *Calphad* **2018**, *62*, 99-108. DOI
76. Zhang, C.; Du, Y.; Liu, S.; Liu, Y.; Sundman, B. Thermal conductivity of Al–Cu–Mg–Si alloys: experimental measurement and CALPHAD modeling. *Thermochim. Acta.* **2016**, *635*, 8-16. DOI
77. Du, B.; Tan, J.; Wu, Q.; Wen, S.; Liu, Y.; Du, Y. Assessment of thermal conductivity for FCC Al-X (X=Zn, Mg) and Al-Zn-Mg alloys: experiments and modeling. *Calphad* **2024**, *87*, 102763. DOI
78. Li, H.; Xu, W.; Zhang, Y.; et al. Prediction of the thermal conductivity of Mg-Al-La alloys by CALPHAD method. *Int. J. Miner. Metall. Mater.* **2024**, *31*, 129-37. DOI
79. Cui, Y.; Li, S.; Ying, T.; Bao, H.; Zeng, X. Research on the thermal conductivity of metals based on first principles. *Acta. Metall. Sin.* **2021**, *57*, 375-84. DOI
80. Sun, Y.; Yang, A.; Duan, Y.; Qi, H.; Peng, M.; Shen, L. Structural stability, elasticity and minimum thermal conductivity of M-doped $Mg_{17}Al_{12}$ (M = Ga, In, Ge, Sn, Pb) compounds: a first-principles predictions. *Int. J. Quantum. Chem.* **2023**, *123*, e27061. DOI
81. Mcgaughey, A. J. H.; Jain, A.; Kim, H.; Fu, B. Phonon properties and thermal conductivity from first principles, lattice dynamics, and the Boltzmann transport equation. *J. Appl. Phys.* **2019**, *125*, 011101. DOI
82. Muthaiah, R.; Garg, J. Thermal conductivity of magnesium selenide (MgSe) - a first principles study. *Comput. Mater. Sci.* **2021**, *198*, 110679. DOI
83. Zhang, X.; Wang, A.; Shao, C.; Bao, H. Understanding thermal transport in magnesium solid solutions through first-principles approaches and machine learning feature screening. *Acta. Mater.* **2024**, *276*, 120160. DOI

84. Zhu, S.; Sarıtürk, D.; Arróyave, R. Accelerating CALPHAD-based phase diagram predictions in complex alloys using universal machine learning potentials: opportunities and challenges. *Acta. Mater.* **2025**, *286*, 120747. DOI
85. Gao, J.; Zhong, J.; Liu, G.; et al. Accelerated discovery of high-performance Al-Si-Mg-Sc casting alloys by integrating active learning with high-throughput CALPHAD calculations. *Sci. Technol. Adv. Mater.* **2023**, *24*, 2196242. DOI PubMed PMC
86. Zeng, Y.; Man, M.; Koon, Ng. C.; et al. Search for eutectic high entropy alloys by integrating high-throughput CALPHAD, machine learning and experiments. *Mater. Design.* **2024**, *241*, 112929. DOI
87. Chen, J.; Zhang, Y.; Luan, J.; et al. Prediction of thermal conductivity in multi-component magnesium alloys based on machine learning and multiscale computation. *J. Mater. Inf.* **2025**, *5*, 22. DOI
88. Chen, J.; Luan, J.; Jiang, S.; Yu, Z.; Fan, Y.; Chou, K. Analytical equations for thermal and electrical conductivity prediction in as-cast magnesium alloys: a symbolic regression approach. *J. Magnes. Alloys.* **2026**, *14*, 101840. DOI
89. Dong, X.; Feng, L.; Wang, S.; et al. A quantitative strategy for achieving the high thermal conductivity of die-cast Mg-Al-based alloys. *Materialia* **2022**, *22*, 101426. DOI
90. Zhang, R.; Song, H.; Zhang, M.; Tian, Y.; Chen, L. CALPHAD simulation and experimental study on heat treatment process of Al-Cu-Mn-Mg-Sc cast alloys. *Mater. Today. Commun.* **2024**, *39*, 108699. DOI
91. Tian, G.; Wang, J.; Xue, C.; Yang, X.; Wang, S.; Su, H. Ultra-light Mg–Li alloy by design to achieve unprecedented high stiffness using the CALPHAD approach. *Calphad* **2023**, *81*, 102556. DOI
92. Chen, Y.; Wang, J.; Zheng, W.; et al. CALPHAD-guided design of Mg-Y-Al alloy with improved strength and ductility via regulating the LPSO phase. *Acta. Mater.* **2024**, *263*, 119521. DOI
93. Zuo, E.; Dou, X.; Chen, Y.; et al. Electronic work function, surface energy and electronic properties of binary Mg-Y and Mg-Al alloys: a DFT study. *Surf. Sci.* **2021**, *712*, 121880. DOI
94. Ju, S.; Yang, C. Understanding the structural, mechanical, thermal, and electronic properties of MgCa bulk metallic glasses by molecular dynamics simulation and density functional theory calculation. *Comput. Mater. Sci.* **2018**, *154*, 256-65. DOI
95. Zhu, W.; Ma, X.; Wang, Y.; Wang, C.; Li, W. First-principles study of the mechanical and thermodynamic properties of aluminium-doped magnesium alloys. *RSC. Adv.* **2024**, *14*, 11877-84. DOI PubMed PMC
96. Liu, W.; Li, Y.; Qiu, J.; et al. Strength-thermal conductivity synergy of aluminum alloys revealed by Al–RE (RE = Ce, La, Gd, Y, Sm, Yb, Er) intermetallic compounds. *Mater. Design.* **2025**, *255*, 114221. DOI
97. Wang, M.; Zhou, Y.; Tian, W.; et al. First-principles study the mechanical, electronic, and thermodynamic properties of Mg-Al-Mn ternary compounds. *Vacuum* **2023**, *213*, 112140. DOI
98. Wang, S.; Zhao, Y.; Guo, H.; Lan, F.; Hou, H. Mechanical and thermal conductivity properties of enhanced phases in Mg-Zn-Zr system from first principles. *Materials* **2018**, *11*, 2010. DOI PubMed PMC
99. Diao, Y.; Yan, L.; Gao, K. A strategy assisted machine learning to process multi-objective optimization for improving mechanical properties of carbon steels. *J. Mater. Sci. Technol.* **2022**, *109*, 86-93. DOI
100. Oh, J. M.; Narayana, P.; Hong, J.; et al. Property optimization of TRIP Ti alloys based on artificial neural network. *J. Alloys. Compd.* **2021**, *884*, 161029. DOI
101. Häse, F.; Roch, L. M.; Aspuru-Guzik, A. Chimera: enabling hierarchy based multi-objective optimization for self-driving laboratories. *Chem. Sci.* **2018**, *9*, 7642-55. DOI PubMed PMC
102. Gou, W.; Shi, Z.; Zhu, Y.; et al. Multi-objective optimization of three mechanical properties of Mg alloys through machine learning. *Mater. Genome. Eng. Adv.* **2024**, *2*, e54. DOI
103. Zhang, P.; Qian, Y.; Qian, Q. Multi-objective optimization for materials design with improved NSGA-II. *Mater. Today. Commun.* **2021**, *28*, 102709. DOI
104. Mo, R.; Wu, L.; Wang, G.; Wang, Q.; Ren, J. Multi-objective optimization of multi-principal element alloys via high-throughput simulation and active learning. *Mater. Today. Commun.* **2024**, *40*, 109731. DOI
105. Chen, Y.; Tian, Y.; Zhou, Y.; et al. Machine learning assisted multi-objective optimization for materials processing parameters: a case study in Mg alloy. *J. Alloys. Compd.* **2020**, *844*, 156159. DOI
106. Liu, H.; Nakata, T.; Xu, C.; et al. Machine learning assisted design of high thermal conductivity and high strength Mg alloys. *Metall. Mater. Trans. A.* **2025**, *56*, 1534-51. DOI
107. Kelsy, B. T.; Nwobi-Okoye, C. C.; Ezechukwu, V. C.; Uche, R. Multi objective optimization of novel Al-Si-Mg nanocomposites: a Taguchi-ANN-NSGA-II approach. *J. Eng. Res.* **2025**, *13*, 267-82. DOI
108. Li, S.; Dong, Z.; Jin, J.; et al. Optimal design of high-performance rare-earth-free wrought magnesium alloys using machine learning. *Mater. Genome. Eng. Adv.* **2024**, *2*, e45. DOI
109. Alaneme, K. K.; Okotete, E. A. Enhancing plastic deformability of Mg and its alloys - a review of traditional and nascent developments. *J. Magnes. Alloys.* **2017**, *5*, 460-75. DOI

110. Ghorbani, M.; Boley, M.; Nakashima, P.; Birbilis, N. A machine learning approach for accelerated design of magnesium alloys. Part B: Regression and property prediction. *J. Magnes. Alloys.* **2023**, *11*, 4197-205. DOI

111. Dong, S.; Wang, Y.; Li, J.; Li, Y.; Wang, L.; Zhang, J. Machine learning aided prediction and design for the mechanical properties of magnesium alloys. *Met. Mater. Int.* **2024**, *30*, 593-606. DOI